Synthesis and evaluation of novel cyclopentane urea FPR2 agonists and their potential application in the treatment of cardiovascular inflammation

Monika Maciuszek [a, b, *], Almudena Ortega-Gomez [c], Sanne L. Maas [c], Mauro Perretti [b], Andy Merritt [a], Oliver Soehnlein [c, d, e], Timothy M. Chapman [a]

[a] LifeArc, Accelerator Building, Open Innovation Campus, Stevenage, UK
[b] The William Harvey Research Institute, Barts and the London School of Medicine, Queen Mary University of London, London, UK
[c] Institute for Cardiovascular Prevention (IPEK), LMU Munich Hospital, Munich, Germany
[d] Department of Physiology and Pharmacology (FyFa), Karolinska Institute, Stockholm, Sweden
[e] German Center for Cardiovascular Research (DZHK), Partner Site Munich Heart Alliance (MHA), Munich, Germany

ARTICLE INFO

ABSTRACT

The discovery of natural specialized pro-resolving mediators and their corresponding receptors, such as formyl peptide receptor 2 (FPR2), indicated that resolution of inflammation (RoI) is an active process which could be harnessed for innovative approaches to tame pathologies with underlying chronic inflammation. In this work, homology modelling, molecular docking and pharmacophore studies were deployed to assist the rationalization of the structure-activity relationships of known FPR2 agonists. The developed pharmacophore hypothesis was then used in parallel with the homology model for the design of novel ligand structures and in virtual screening. In the first round of optimization compound **8,** with a cyclopentane core, was chosen as the most promising agonist (β-arrestin recruitment $EC_{50} = 20$ nM and calcium mobilization $EC_{50} = 740$ nM). In a human neutrophil static adhesion assay, compound **8** decreased the number of adherent neutrophils in a concentration dependent manner. Further investigation led to the more rigid cycloleucines (compound **22** and **24**) with improved ADME profiles and maintaining FPR2 activity. Overall, we identified novel cyclopentane urea FPR2 agonists with promising ADMET profiles and the ability to suppress the inflammatory process by inhibiting the neutrophil adhesion cascade, which indicates their anti-inflammatory and pro-resolving properties.

1. Introduction

Currently there is increased interest in the exploitation of the processes that characterise the resolution phase of inflammation [1–4]. It is a novel approach, hence developing modulators as an effector of resolution has the potential to treat not only the cardiovascular inflammatory pathologies [5–7], but also for example bowel disease [8], chronic obstructive pulmonary disease (COPD) [9–11], rheumatoid arthritis [12,13], Alzheimer's Disease [14], neuroinflammation [15–17] and allergies [18]. FPR2 is a target of interest for pro-resolving treatment of chronic inflammation. FPR2 is a G-protein coupled receptor which is highly expressed in neutrophils [19–23] and monocytes [24,25] but it can also be located on the surface of various types of cells for example endothelia, epithelia and smooth muscle cells. FPR2 can be activated by agonists of diverse origins such as lipid (LXA$_4$ [23,25–28], Resolvin D1 [29–31]), proteins (Annexin A1 [AnxA1] [11,24]), synthetic peptides (WKYMV [32,33]) and small molecule ligands (Compound 43 [7,34]). Depending on the nature of the agonist, FPR2 can have a dual effect on the inflammatory response [2]. As an example, activation of FPR2 by serum amyloid A (SAA) triggers pro-inflammatory responses [35,36]. On the other hand, activation of FPR2 by pro-resolving mediators such as lipoxin A$_4$ (LXA$_4$), resolvin D1 or AnxA1 enables the cascade of anti-inflammatory and pro-resolving responses e.g. inhibition of neutrophil trafficking and transmigration and promotion of macrophage-mediated phagocytosis [1,4,7,37]. Current efforts are focused on untangling the complexity of this receptor. In 2012 Perretti et al. created FPR1/

* Corresponding author. LifeArc, Accelerator Building Open Innovation Campus, Stevenage, UK.
E-mail address: maciuszekmonika@gmail.com (M. Maciuszek).

FPR2 chimera proteins to determine the regions which are important for FPR2 receptor activation using AnxA1, SAA and Compound 43 [38]. The extracellular loop I, transmembrane region III and intracellular loop II were identified as the domains taking part in the binding of small molecule agonist Compound 43. From mutagenesis studies and later docking studies, four amino acid residues (Arg-26, Asp-106, Arg-205 and Asp-281) were suggested as important for the binding of peptide agonists [39,40]. In 2020 the first crystal structure of human FPR2 in complex with WKYMVm was published [41]. These discoveries increased our knowledge regarding ligand recognition and possible binding modes of the formyl peptide receptor ligands. In the last 10 years research groups have focused on pro-resolving properties of the FPR2 receptor and several synthetic small molecules have been submitted for Phase I clinical trials [42,43], but none of them has yet become the first-in-class pro-resolving drug. Nevertheless, each synthesized small molecule agonist has made its contribution to the progress in pharmacology and molecular biology of FPR2. In this work, we demonstrate that homology modelling, followed by a combination of ligand and structure-based design employing bioisosteric replacement and synthesis, supported with ADME profiling is a rational option for the development of novel agonists. Using this approach various N-urea-substituted non-natural amino acids moieties were explored. All synthesized compounds were assessed for their agonistic activity to induce calcium mobilization and β-arrestin recruitment in CHO−K1 FPRL1 cells (DISCOVERx) overexpressing hFPR2. Moreover, all synthesized compounds were assessed in *in vitro* absorption, distribution, metabolism and excretion and toxicity (ADMET) assays such as kinetic solubility and microsomal stability to bring better insight to their potential for further development.

2. Results and discussion

2.1. In silico studies

In these studies, a 'ready-to-use' homology model was adopted: an agonist (BU72) bound μ-opioid based structure (5C1M) [44] from GPCRdb [45], allowing us to develop a hypothesis for the binding sites of the ligands. Sitemap was used to predict possible druggable regions in the receptor with the volume 641.5 Å^3. In order to predict probable binding modes, compounds with known agonistic properties were selected from literature based on their activity and the diversity of the chemical structures. For this purpose, six key families were chosen to explore possible binding poses: pyrazolone urea [46,47], N-urea-substituted amino acids [48−51], oxazoles [52−54], N-urea-substituted furans [55], bridged spiro[2.4] heptanes [56−58] and pyridazinones [59,60]. All literature EC_{50} values presented are from the calcium mobilization assays. In the figure below representative compounds with their chemical structures used in modelling the active site of FPR2 are presented (Fig. 1).

The final receptor grid generation was performed using the results from SiteMap using the Glide SP-protocol. To facilitate the examination of the receptor grid, test virtual screening of actives and decoys was performed. The decoys were generated for known active agonists using the DUDE database. The enrichment factor was calculated, and the value of receiver operating characteristic (ROC) was 0.70 with all active molecules placed in the first 35% of screened compounds. These results gave us confidence that we can distinguish actives from inactive compounds. This model highlighted the concept of the binding pocket made up with three hydrophobic subpockets with two polar clusters. FPR2 agonists do not need to occupy all three proposed subpockets (Fig. 2). Analysis of the binding modes showed that for each molecule an important

aromatic stacking was observed with at least one of the amino residues: Phe-257, Phe-292, Phe-163, Tyr-175 and His-102. This concept corresponds partially with binding modes suggested by research groups from Montana University and Warsaw University [35,39,61]. In all six families, the hydrophobic pocket I is always occupied by a phenyl ring or in the case of compound **5** by the bridged spiro[2.4]heptane core and they make π-π stacking and hydrophobic interactions. The urea or amide groups in compounds **1**−**5** occupy polar clusters in the active site and form hydrogen bonding interactions with the backbone of amino acid residues such as Cys-179, Ser-288 or His-102.

Development of a pharmacophore hypothesis was performed using the Phase tool in Schrödinger Maestro. The five-point pharmacophore hypothesis has been chosen among 32 hypotheses with PhaseHypoScore equals 1.17 and ROC value 0.9. This pharmacophore model emphasized a substituted ring (Ring R9) at the *para* position, preferably with a lipophilic and electronegative moiety, for instance halogens (Hydrophobic H6). The results from the pharmacophore studies established the importance of the NH moiety (Donor D4) and the oxygen atom from the carbonyl group (Acceptor A3). The hydrophobic feature (H8) covers alkyl chains and the three-dimensional cores of the bridged spiro[2.4]heptane derivatives and the Kyorin compounds. A pharmacophore model derived from the binding modes of the FPR2 agonists in the homology model studies is shown in Fig. 3.

2.2. Design and development of novel agonists

Following the development of both the homology and pharmacophore models, they were then deployed in the search for novel ligands. As the starting point we proposed compound **7** with an ʟ-leucine motif (R1) which is known from the N-urea-substituted amino acids [48−51], the largest family of FPR2 agonists developed by Allergan. From the *in silico* studies performed (section 2.1) we observed that the ʟ-leucine alkyl chain is located in the cavity formed with Met-85, Ser-84, Leu-81 and stabilizes the ligand in the pocket. The presence of an aromatic ring in the R2 position is common for FPR2 agonists (Fig. 1: 1 and 4). We decided to use a 3-pyridyl group (R2) as the starting point in order to add a weakly basic centre. Analysis of the binding modes showed that the 3-pyridyl ring was oriented towards the solvent-exposed space in subpocket 2, suggesting there may be scope to further vary this group to tune the physicochemical properties. A series of urea compounds was designed and synthesized via introducing an alkyl or cyclic moiety as replacements for ʟ-leucine. For this purpose, commercially available unnatural amino acids were chosen. We decided to maintain two key structural features: the urea moiety and the *para*-bromo substituted phenyl ring, as both play an important role in the ligand binding according to the *in silico* studies (Fig. 4).

When a ligand activates the receptor, it might trigger the G-protein and/or β-arrestin signalling cascade. Accordingly, in this study two functional assays were adopted: β-arrestin recruitment and calcium mobilization. In the calcium mobilization assay we measure the release of calcium from the endoplasmic reticulum driven by activation of the G-protein. Using both assays we were able to determine if the developed ligands are balanced agonists, G-protein biased agonists or β-arrestin biased agonists. The results from the β-arrestin and calcium mobilization assays revealed the importance of a bulky substituent at R1 in order to retain the activity. With R1 as hydrogen (**6**), this compound is completely inactive in the β-arrestin assay, and in calcium mobilization the EC_{50} value is 0.73 μM, however the efficacy (E_{max}) is below 50%. Our starting molecule, compound **7,** only partially activated the receptor in both cellular assays, though it has good metabolic stability
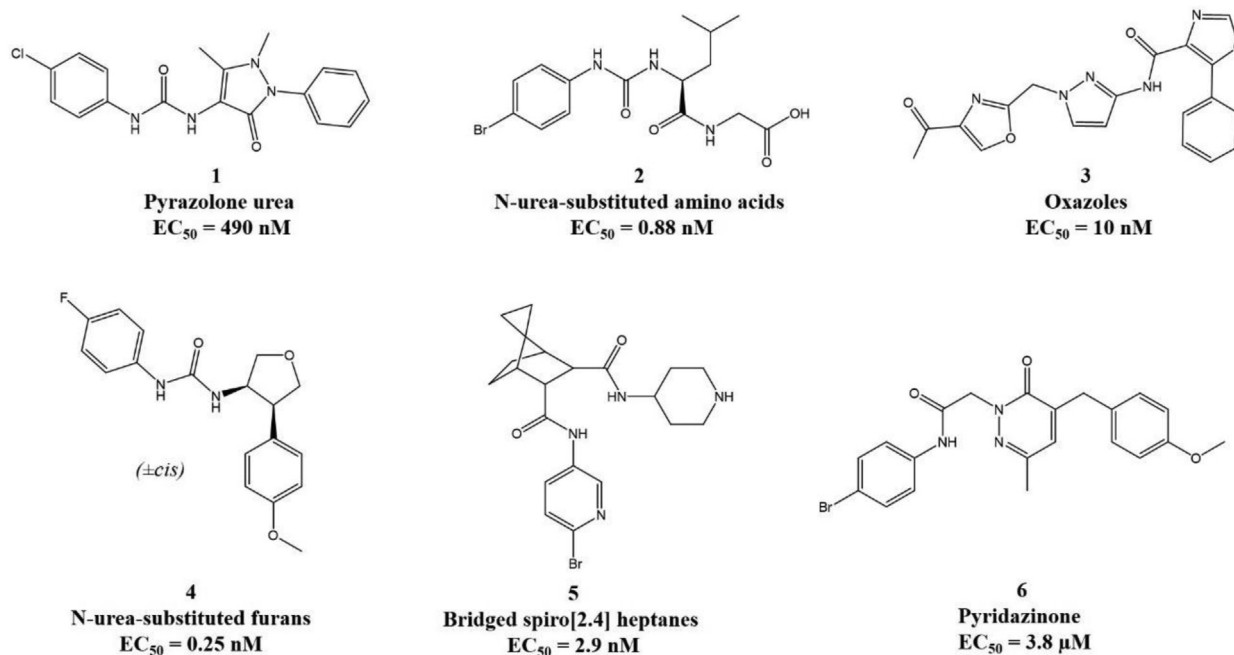
Fig. 1. Selected examples of the existing FPR2 small molecule agonists used in in silico studies
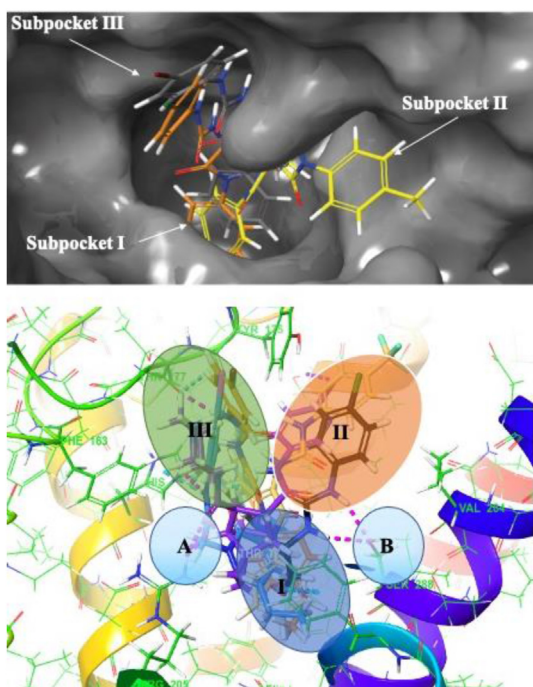All literature EC_{50} values presented are from calcium mobilization assays.

Fig. 2. Model of the compounds (Allergan urea and pyrazolone) docked to FPR2 and proposed three hydrophobic subpockets model with two polar clusters.

Fig. 3. The five-point pharmacophore hypothesis.

and reasonable kinetic solubility. In the calcium mobilization assay ligands **8** and **10**−**12** exhibited full agonistic efficacy, showing that these cyclic alkyl substituents have a positive effect, and this supports our finding from docking studies. Among the newly developed ligands, compound **8** exhibited the best overall FPR2 activation profile across both functional assays at sub-micromolar
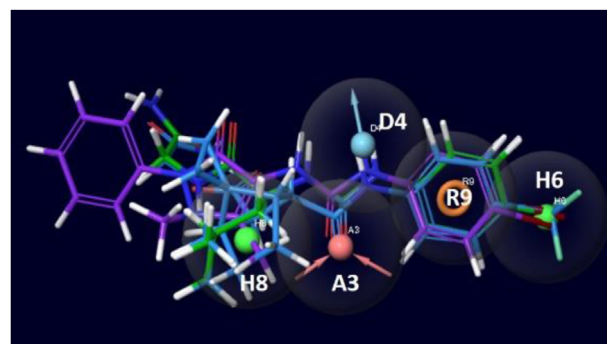
concentrations. Various non-natural amino acid cores are well tolerated in the microsomal stability assays, showing good stability in human liver microsomes (HLM). Introduction of a larger substituent than cyclopentane **8**, for example tetrahydropyran **9** or methylcyclohexyl **10** led to reduced efficacy or a decrease in agonist potency in calcium mobilization, respectively. Moreover, the structural modifications in compound **10** had a negative effect on metabolic stability and kinetic solubility. Overall, the cyclopentane **8**, methylcyclopropyl **11** and cyclopropyl **12** have promising in vitro ADME profiles which can serve as a good basis for further optimization (Table 1).

Compound **8** was chosen for further structural modification due to its balance of potency, efficacy, and properties. Furthermore, positive results from human neutrophil adhesion assays demonstrated the anti-inflammatory properties of compound **8**, so this was an additional factor which fed into the selection [data are presented in section 2.4]. Attention turned to replacement of the aromatic amine with more hydrophilic moieties (Table 2). The azetidine **14** and methyl-piperidine **15** showed markedly better kinetic solubility and LogD values, though simultaneously we
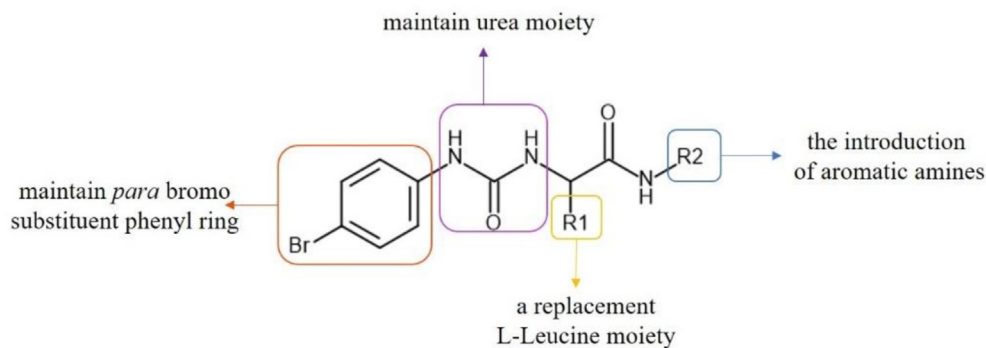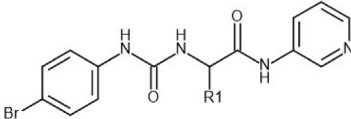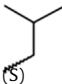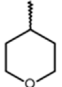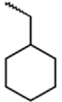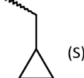
Fig. 4. Starting point for the design and development of novel FPR2 agonists

Table 1
ADME properties and EC$_{50}$ values for urea derivatives.

ID	R1	Kinetic Solubility [μM]	LogD[a]	Microsomal stability				Ca^{2+} EC$_{50}$ [μM][f] (E$_{max}$/%[g])	β-arrestin EC$_{50}$ [μM][f] (E$_{max}$/%[g])
				t$_{1/2}$ [min][b]		CL$_{int}$[c] [μL/min/mg]			
				HLM[d]	MLM[e]	HLM[d]	MLM[e]		
6	-H	27	3.6	112	22	14	71	0.73 (49)	NA
7	(S)	34	4.2	95	65	16	24	0.03 (38)	4.26 (82)
8	cyclopentyl	17	>4	83	33	19	47	0.02 (137)	0.74 (98)
9	tetrahydropyran	32	4.7	188	90	8	17	0.072 (77)	4.17 (93)
10	cyclohexylmethyl	0	>4	61	11	25	142	1.3 (150)	2.15 (77)
11	cyclopropyl (S)	11	>4	91	44	17	35	0.068 (90)	1.35
12	cyclopropyl	41	>4	80	41	19	38	0.097 (100)	7.8 (93)
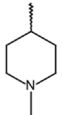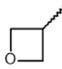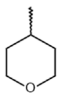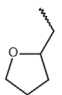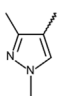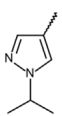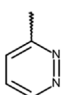
NA - very low response (E$_{max}$ <30% of max response) or weak activation EC$_{50}$ > 10 μM.
[a] LogD - distribution coefficient.
[b] t$_{1/2}$ − half-life [min].
[c] Clint - intrinsic clearance [μL/min/mg].
[d] HLM - human liver microsomes.
[e] MLM - mouse liver microsomes.
[f] EC$_{50}$ - half maximal effective concentration [μM].
[g] E$_{max}$ efficacy- [%]

observed a drop-off in potency. Additionally, the 3-pyridine (**8**) was exchanged for cyclic ethers: oxetane (**16**), tetrahydropyran (**17**) and 2-methyltetrahydrofuran (**18**). The cyclic ether analogues displayed good microsomal stability, except **18** which is extremely unstable. The cyclic ether analogues **16**–**18** exhibit sub-micromolar activity in the calcium mobilization assay, however only **18** had the ability
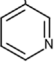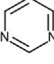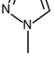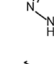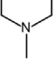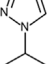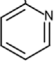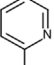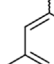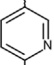
Table 2
Summary showing ADME properties and EC$_{50}$ values of selected compounds from cyclopentyl-acetamide series.

ID	R2	Ks [μM]	LogD[a]	T$_{1/2}$[b] [min]		Clint[c] (μL/min/mg)		Ca^{2+} EC$_{50}$ [μM][f] (E$_{max}$/%)[g]	β-arrestin recruitment EC$_{50}$ [μM][f] (E$_{max}$/%)[g]
				HLM[d]	MLM[e]	HLM[d]	MLM[e]		
8		17	>4	83	33	19	47	0.02 (100)	0.74 (98)
13		47	4	184	92	8	17	0.8 (120)	6.33 (100)
14		178	1.6	121	65	13	24	3.85	0.50 (97)
15		200	2.5	110	477	14	3	3.67 (130)	NA
16		26	4.3	>400	>400	<3	<3	0.62 (95)	NA
17		1	>4	207	104	7	14	0.6 (132)	NA
18		22	4.7	13	25	121	62	0.54 (96)	0.94 (101)
19		0	>4	72	83	22	19	0.48 (100)	1.9 (86)
20		0	>4	55	12	28	126	1.24 (111)	7.45 (43)
21		59	>4	16	11	99	133	0.07 (68)	1.41 (84)

NA - very low response (Emax <30% of max response) or weak activation EC$_{50}$ > 10 μM.
[a] LogD - distribution coefficient.
[b] t$_{1/2}$ − half-life [min].
[c] Clint - intrinsic clearance [μL/min/mg].
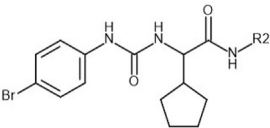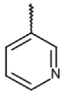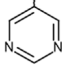[d] HLM - human liver microsomes.
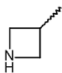[e] MLM - mouse liver microsomes.
[f] EC$_{50}$ - half maximal effective concentration [μM].
[g] E$_{max}$ efficacy- [%].

Table 3
Summary showing ADME properties and EC_{50} values of selected compounds from cycloleucine series.

ID	R2	Ks [μM]	LogD[a]	$T_{1/2}$ [min][b]			Cl_{int} (μL/min/mg)[c]			Ca^{2+} EC_{50} [μM][f] (E_{max})[g]	β-arrestin recruitment EC_{50} [μM][f] (E_{max})[g]
				HLM	HLM[d]	MLM[e]	HLM	HLM[d]	MLM[e]		
22		103	4.1	108	108	79	14	14	19	0.250 (110)	1.3 (99)
23		214	3.7	110	110	104	14	14	15	0.366 (90)	7.27 (92)
24		225	3.1	156	156	227	10	10	7	0.089 (86)	1.85 (89)
25		223	1.1	520	520	419	3	3	4	0.272 (88)	NA
26		226	1.2	157	157	194	10	10	7.9	1.6 (95)	NA
27		33	4.2	130	130	90	12	12	17	1.1 (96)	4.15 (51)
28		43	4.3	8	8	9	186	186	180	6.07 (49)	NA
29		31	3.9	100	100	36	16	16	42	0.60 (68)	9.9 (60)
30		30	3.7	86	86	39	18	18	39	1.75 (79)	9.8 (60)
31		0	4.4	52	52	32	30	30	47	0.11 (60)	2.58 (71)

NA - very low response (Emax <30% of max response) or weak activation EC_{50} > 10 μM.
[a] LogD - distribution coefficient.
[b] $t_{1/2}$ − half-life [min].
[c] Clint - intrinsic clearance [μL/min/mg].
[d] HLM - human liver microsomes.
[e] MLM - mouse liver microsomes.
[f] EC_{50} - half maximal effective concentration [μM].
[g] E_{max} efficacy- [%].

to activate FPR2 through the β-arrestin pathway (EC_{50} = 0.95 μM). The distinct difference in metabolic stability with **18** suggests that either a CH_2 in the tetrahydrofuran ring or the −CH_2 linker can act as a metabolic soft-spot in this example. Based on the observed SAR, it was decided to synthesise three additional analogues of **8** with the pyridine replaced by alternative heterocycles. This included pyrazole variants (**19**−**20**) and pyridazine (**21**), which were expected to represent a good compromise for the overall
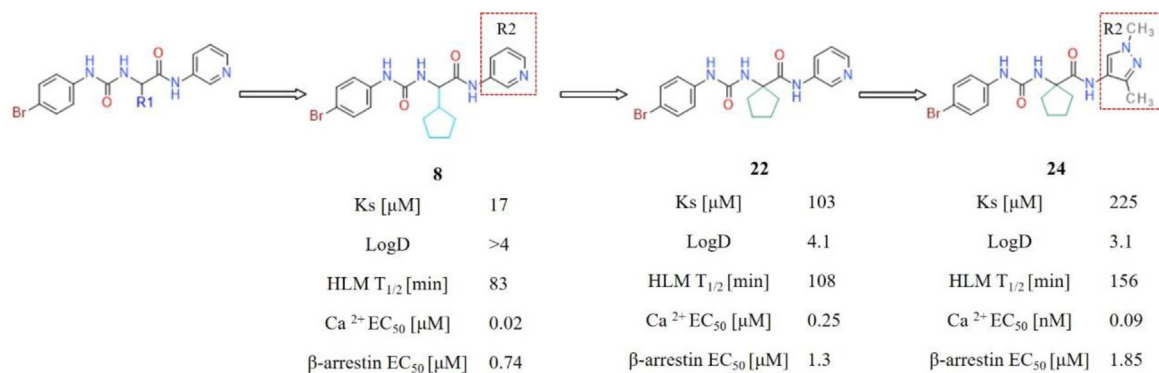
Fig. 5. Optimization of cyclopentane urea FPR2 agonists.

molecular properties. The pyrazole derivatives **19** and **20** were less active than compound **8**, however both ligands exhibit low micromolar potency in the calcium mobilization assay (Ca^{2+} EC_{50} = 0.481 and 1.24 μM respectively). The dimethylpyrazole analogue **19** showed moderate microsomal stability, however both **19** and **20** suffered from poor solubility. The pyridazine **21** was the most active amongst these three modifications, nevertheless it experiences a low metabolic stability. Compound **21** undergoes a rapid *in vitro* intrinsic clearance in comparison to pyrimidine compound **13** (HLM/MLM Cl_{int} 8/13 μL/min/mg). The additional nitrogen atom in the ring (**13** Ks = 47 μM and **21** Ks = 59 μM) improves the kinetic solubility compared to **8** (Ks = 17 μM), nevertheless it has a negative impact on activity. (Table 2). In summary, the aromatic ring at the R2 position appears to be beneficial but it is not absolutely crucial to maintaining agonistic activity.

On the basis of the results described above, the next step was further improvement of the scaffold. It was decided to introduce a geminally substituted cyclopentane ring to the alpha-C atom of the amino acid. Gratifyingly, this cycloleucine series showed significantly improved solubility and the potency was maintained in the nanomolar range in calcium mobilization (Table 3, **22**−**23**). The SAR studies were then focused on the replacement of pyridine ring. The dimethylpyrazole **24** has a low clearance amongst both species with LogD slightly above 3, increased kinetic solubility and improved activity in the calcium mobilization assay. Another compound with an encouraging profile is the tetrazole **25**: the acidic proton of the tetrazole results in low log D, high metabolic stability and high solubility; however, compared to **24**, it is 4-fold weaker in calcium mobilization (272 nM) and inactive in the β-arrestin assay. The weaker performance of the 1-isopropyl-1H-pyrazole **27** in the functional assays could be justified by steric clashes compared to **24** and **25**. Compound **28**, containing the 2-pyridine, showed weaker potency and approximately a 10-fold shorter half-life than **22**, highlighting the 3-pyridine's superior stability. The 1-methylpiperidine derivative **26** was synthesized to study the impact of non-aromatic rings on the agonistic activity. The outcome correlates with the results for the cyclopentyl-acetamide series, where substitution of the aromatic ring for an alicyclic group caused a drop-off in activity. Introduction of a methyl group adjacent to the pyridine nitrogen (**29**) reduced solubility and stability in MLM, but still sustained activity in the nanomolar range. By contrast a methyl group at the pyridine 3-position (**30**) led to a significant drop-off in activity in the calcium mobilization assay. Replacing this methyl with a chlorine (**31**) led to improved activity in the calcium mobilization assay (EC_{50} = 107 nM) although it suffers from poor solubility (Table 3). Although compounds **29**−**31** display promising stability in HLM, their stability is significantly lower in MLM.

In summary, as the starting point we proposed compound **7** with an L-leucine core, which is known from N-urea-substituted amino acids [48−51]. Investigation of alternative R1 substituents based on compound **7** resulted in the enhancement of the FPR2 agonistic activity. Compound **8** was chosen for further structural modification due to its balance of potency, efficacy, and properties. In the next step of optimization, we introduced a geminally substituted cyclopentane ring (**22**). Finally, re-optimization of the R2 position with this core in place led to the identification of the dimethylpyrazole-substituted example **24** (Fig. 5). For the leading compounds, in order to determine whether any cytotoxic effects are observed, a cell health assay was performed using HepG2 cells, a human hepatocyte carcinoma line. None of the compounds appeared to show any signs of toxicity at any of the parameters tested up to 30 μM (**supplementary data**).

2.3. Chemistry

Pathway 1 was used when starting with the alpha amino acid ester and commercially available 4-bromophenyl isocyanate **33** to obtain the urea derivatives **34**−**40** with good yield. Cleavage of the ester group with formic acid or 2M aqueous solution of sodium hydroxide at room temperature generated an acid **41**−**47** in quantitative yield. Final amide coupling was performed in the presence of triethylamine and T3P as a coupling agent **7**−**10**; **13**, **15**−**31** and **48**. When the alpha amino acid ester is not available pathway 2 was used, the first step was amide coupling with the BOC-protected amino acid **49**−**50** in the presence of triethylamine and T3P as a coupling agent. Then deprotection of BOC protected amine was performed using 4M HCl in dioxane in quantitative yield. Finally, the urea derivative **11**−**12** was obtained in the coupling with 4-bromophenyl isocyanate (Scheme 1).

2.4. Determination of the anti-inflammatory properties of the FPR2 agonists

To assess their possible therapeutic activity for the treatment of cardiovascular inflammatory diseases, a human neutrophil static adhesion assay was performed on the leading compounds.

Fig. 6 shows the results obtained from profiling two known active FPR2 agonists. They were used as a benchmark for the novel agonists. Compound **2**, which is one of the Allergan small molecule agonists described in patent application US20170320897 covering treatment of ocular inflammation, showed good inhibition of neutrophil adhesion. The second compound is Compound 43 (**32**), developed by Amgen, which also shows anti-inflammatory properties in a dose-dependent manner (Fig. 6).

The functional assays described earlier had shown that in the non-natural amino acid series, the presence of a bulky substituent
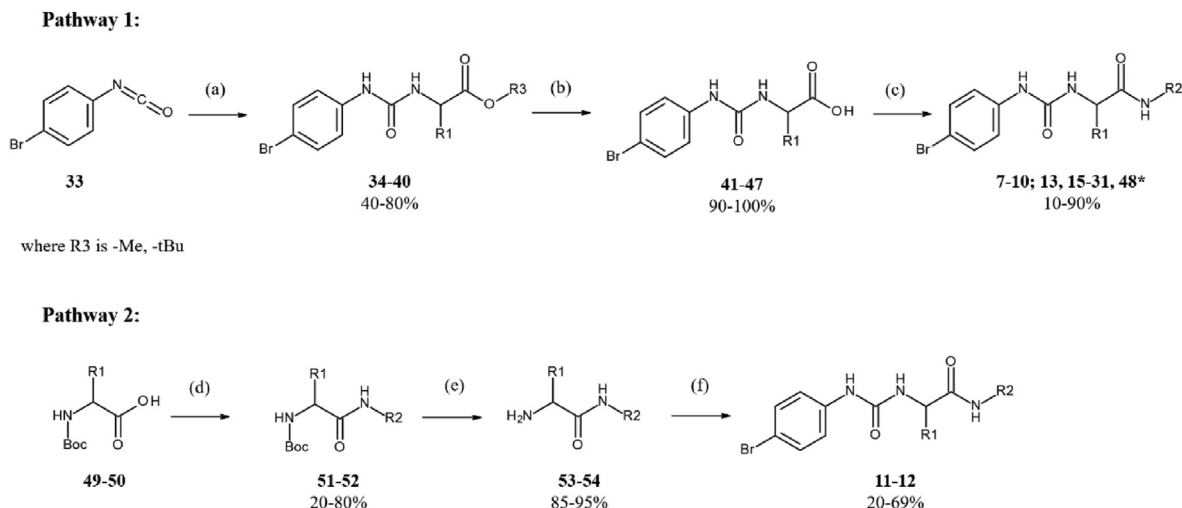
Scheme 1. Two synthetic pathways used for non-natural amino acid series. Conditions: Pathway 1: (a) 1 eq. amino acid., 1.5 eq. TEA, DCM, RT, 4 h; (b) formic acid, RT, 4 h; (c) 1.5 eq T3P, 1.1 eq. amine, ethyl acetate, RT, overnight; * in addition compound **48** was deprotected to form compound **14** using 4M HCl in dioxane, DCM, RT 4 h; Pathway 2: (d) 1.5 eq T3P, 1.1 eq. amine, ethyl acetate, RT, overnight; (e) 4M HCl in dioxane, DCM, 0 °C to RT, 2–4 h or overnight; (f) 1.2 eq. 4-bromophenyl isocyanate., 1.5 eq. TEA, DCM, RT, 4 h.

in the position R1 is crucial to maintaining the activity. Leading examples were tested in primary cell assays and in Fig. 6 three selected compounds from this series are presented. The parent L-leucine compound **7** showed around a 50% decrease relative to the control and this value is perpetual across entire concentration range; this could be triggered by desensitization of the receptor. Compound **11**, with the cyclopropylmethyl core, showed minimal reduction of adherent neutrophils. The cyclopentane analogue **8** decreased the number of adherent neutrophils in a concentration dependent manner (Fig. 6) and showed enhanced anti-inflammatory properties compared to compound **7**.

2.5. PK studies

Compound **8** was chosen for pharmacokinetic studies which were performed in male C57BL6 mice with intraperitoneal administration at 10 mg/kg (Table 4). Following a single dose, **8** was rapidly absorbed (T_{max} = 0.5 h), showed a high C_{max}, along with a good half-life (2.08 h) and high exposure (area under the concentration-time curve from 0 to infinity (AUC_{0-inf}) = 68961 ng h/mL).

3. Conclusions

In these studies, novel urea-based FPR2 agonists were designed and a structure-activity relationship study was conducted, based on insights provided from *in silico* studies including homology modelling, docking and pharmacophore studies. Based on the results from the *in silico* studies, the introduction of different moieties in the R1 position, for example alkyl, cycloalkyl and heterocyclic substituents, offered the chance to improve the fit into the binding pocket and gain activity. Compound **8** was chosen for further structural modification due to its balance of potency, efficacy, and properties. Further investigation led to the more rigid cycloleucine (compound **22**). The cycloleucine series resulted in an improvement in solubility and the activity was sustained in the nanomolar or submicromolar range. Leading examples showed good *in vitro* ADMET profiles and no cytotoxicity in HepG2 cells, a human hepatocyte carcinoma cell line. Through building the structure-activity relationships (SAR), we discovered the benefit of an aromatic ring at the R2 position such as 3-pyridine, pyrimidine or substituted pyrazoles. The five-membered rings such as pyrazoles

(**24**) and tetrazoles (**25**) showed the most promising ADME and activity profiles in the cycloleucine series. The dimethylpyrazole-substituted ligand **24** showed reduced lipophilicity (LogD = 3.1), high solubility (Ks = 225 μM) and low *in vitro* intrinsic clearance (HLM/MLM Cl_{int} 10/7 μL/min/mg). Leading exemplars were tested in a static adhesion assay, and compound **8** in particular demonstrated the ability to reduce the neutrophil adhesion to proteins such as P-selectins and ICAM. The binding of anti-inflammatory agonists might prevent binding of the other pro-inflammatory ligands like Serum Amyloid A (SAA), or control release of pro-inflammatory cytokines. Future work will involve testing the later molecules in the static adhesion assays, especially compounds **22** and **24**. Finally, compound **8** also showed a promising PK profile and the small molecule FPR2 agonists described here might be valuable tools for the further study of the molecular mechanisms involved in atherosclerosis or ischemia reperfusion injury.

4. Materials and experimental methods

4.1. In silico studies

Homology model: An agonist bound μ-opioid based structure receptor was acquired from GPCRDB [http://gpcrdb.org/protein/fpr2_human/].

Docking Studies: Protein-Ligand docking was performed using the Glide SP-protocol with an outer box 20x20 × 20 Å. All ligands were treated as flexible molecules. Binding site was identified using by Sitemap (Schrödinger Release 2018-2: Schrödinger, LLC, New York, 2018.) Ligands were prepared and visualized using Maestro 11.5. To generate decoys for active agonists DUDE database (http://dude.docking.org/) was used.

Pharmacophore Studies: Pharmacophore hypothesis was obtained from multiple active ligands using Phase with the 'multiple ligands' option and the method 'best alignment and common features'. (Schrödinger Release 2018-2: Schrödinger, LLC, New York, 2018).

4.2. Chemistry

All reagents were purchased from Sigma-Aldrich, Enamine, Fluorochem and other major suppliers and used without further purification. Solvents were purchased from Fisher Scientific (HPLC
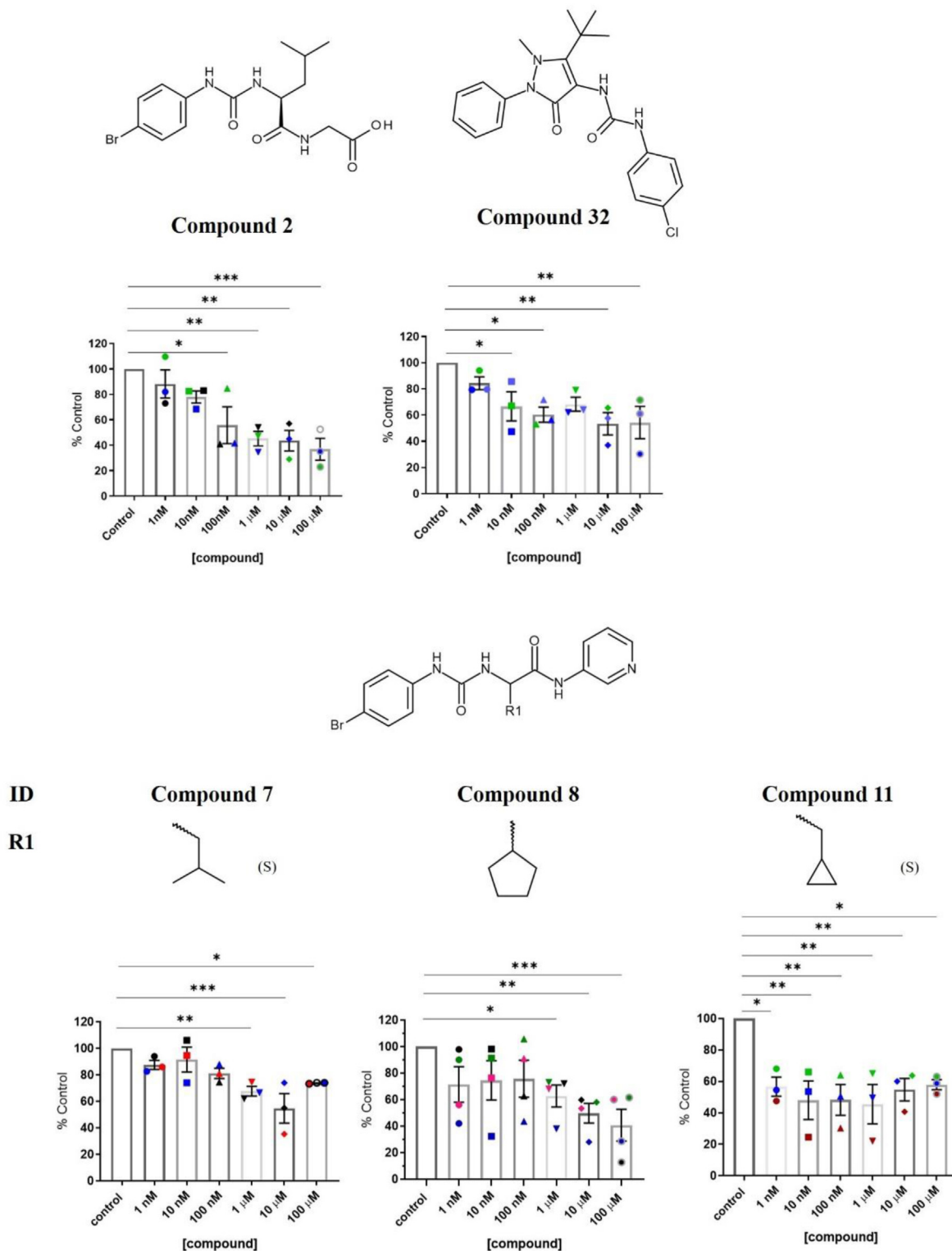
Fig. 6. Anti-adhesive properties of FPR2 agonists 2 (Allergan) and 32 (compound 43) and non-natural amino acids series
All data were shown as means ± SEM., 3–4 independent experiments with 3 technical replicates. The difference between control group, and treatment groups was evaluated via one-way Anova followed by Dunnett's multiple comparison test, and the difference was considered significant for a P value < 0.05: *P < 0.05, **P < 0.01, ***P < 0.001; ns − not significant.

grade) or Sigma-Aldrich (anhydrous). Flash column chromatography was carried out with Biotage KP-Sil Snap cartridges using a Biotage Isolera-One and HPLC grade solvents. Reverse phase column chromatography was carried out on a Biotage Isolera with

prepacked columns of C18 silica and HPLC grade solvents and buffers (Buffer A: 0.1% Ammonium Hydroxide in water; Buffer B: 0.1% Trifluoroacetic acid in water). Purification of compounds by preparative HPLC was carried out on an Agilent Reverse Phase Mass

Table 4
In vivo PK parameters of compound 8 with intraperitoneal administration.

Dose[a]	Cmax[b]	Tmax[c]	$T_{1/2}$[c]	AUC_{0-last}[d]	AUC_{0-inf}[d]	AUC_{Extra}[e]	MRT_{0-last}[c]
10	31905	0.5	2.08	68961	68978	0.02	2.41

[a] Dose is expressed in mg/kg.
[b] C_{max} is expressed in ng/mL.
[c] T_{max}, $T_{1/2}$ and MRT_{0-last} are expressed in hours [h].
[d] AUC_{0-last} and AUC_{0-inf} are expressed in ng·h/mL.
[e] AUC_{0-last} is expressed in %.

Directed Prep HPLC system by a member of the purification team. LC/MS purity analysis was performed on an Agilent 6120 quadrupole LC-MS with an Xbridge C18 column (3.5 μm particle and 4.6 × 30 mm dimension) and a diode array UV detector. Four methods were used depending on the nature of the compound: Method A: flow rate: 3 mL/min; Run time: 3.2 min: Solvent A: 0.1% Trifluoro Acetic acid in water, Solvent B: Acetonitrile; Gradient - 10−100%B; Gradient time: 2.35 min; Method B: flow rate: 3 mL/min; Run time: 3.2 min: Solvent A: 0.1% Ammonium Hydroxide in water, Solvent B: Acetonitrile; Gradient - 10−100%B; Gradient time: 2.35min; Method C: flow rate: 3 mL/min; Run time: 3.2 min: Solvent A: 0.1% Trifluoro Acetic acid in water, Solvent B: Methanol; Gradient - 10−100%B; Gradient time: 2.35min; Method D: flow rate: 3 mL/min; Run time: 3.2 min: Solvent A: 00.1% Ammonium Hydroxide in water, Solvent B: Methanol; Gradient - 10−100%B; Gradient time: 2.35min. HRMS were recorded on a Thermo-Fisher Q-Exactive operating at 70,000 Resolution. NMR solvents were obtained from Cambridge Isotope Labs. All ^{1}H NMR (500 MHz) and ^{13}C NMR (126 MHz) spectra were recorded on a JEOL ECA-500 spectrometer at 21 °C. Chemical shifts (δ) are in ppm and are relative to residual undeuterated NMR solvent. Spectra are referenced to a singlet at 7.27 ppm (CDCl$_3$), the centreline of quintet at 2.50 ppm ((CD$_3$)$_2$SO), quintet at 3.31 ppm (CD$_3$OD) for ^{1}H NMR and to the centreline of a triplet at 77.23 ppm (CDCl$_3$), septet at 39.7 ppm ((CD$_3$)$_2$SO), septet at 49.15 ppm (CD$_3$OD) for ^{13}C NMR. All ^{13}C NMR spectra were proton decoupled. Structural assignments for ^{13}CNMR were denoted as follows: −OCH$_3$ = C atom of methoxy group, C=O = C atom of carbonyl, ArCH = aryl carbon bearing a hydrogen atom, ArC = aryl carbon, Cgem = the alpha-C atom of the amino acid attached directly to cyclopentane, CH = alkenyl carbon, CH$_2$ = methylene carbon, CH$_3$ = methyl carbon, COOH = carbon atom of carboxylic acid, C(CH$_3$)$_3$ = carbon atom of tertbutyl group, C(CH$_3$)$_3$ = tertiary carbon atom of tertbutyl group.

General procedure A for urea formation: Prepared according to the literature procedure [49,50,62]. To a solution of amino acid (1.1 equiv.) in dichloromethane at room temperature was added the appropriate isocyanate (1 equiv.) and triethylamine (1.5 equiv.). The resulting mixture was stirred at room temperature for 3 h. RM was concentrated and purified by flash column chromatography using as an eluent PE/EtOAc to obtain the desired product as white solid.

Tert-butyl 2-[(4-bromophenyl)carbamoylamino]acetate (34) Prepared according to procedure A with intermediate **33** (1 equiv., 3 mmol) and glycine tert-butyl ester hydrochloride (1.1 equiv, 3.3 mmol). Crude product purified by flash column chromatography (silica gel) using PE/EtOAc 1/1. Yield: 460 mg, 90%; Appearance: white solid; LCMS: 1.61 min, *m/z* 330, 332 ((M+H)$^+$ 1:1, $^{79/81}$Br), Purity >95%, Method B ^{1}H NMR (500 MHz, CHLOROFORM-*d*) δ ppm 7.37−7.32 (m, 2 H), 7.13−7.21 (m, 2 H), 5.66 (t, *J* = 5.16 Hz, 1 H), 3.96 (d, *J* = 5.16 Hz, 2 H), 1.47 (s, 9 H); . ^{13}C NMR (126 MHz, DMSO-*d$_6$*) δ ppm 169.91 (1 C, C=O), 155.03 (1 C, C=O), 139.74 (1 C, ArC), 131.42 (2 C, ArCH), 119.63 (2 C, ArCH), 112.55 (1 C, ArC), 80.57 (1 C, C(CH$_3$)$_3$), 41.96 (1 C, CH$_2$), 27.77 (3 C, CH$_3$).

Rac-methyl 2-[(4-bromophenyl)carbamoylamino]-2-cyclopentyl-acetate (35) Prepared according to procedure A with intermediate **33** (3 mmol) and methyl 2-amino-2-cyclopentyl-acetate HCL (1 equiv., 3 mmol); Yield: 640 mg, 70%; Appearance: white solid; LCMS: 1.77 min, *m/z* 356.0, 358.0 ((M+H)$^+$ 1:1, $^{79/81}$Br), Method B; ^{1}H NMR (500 MHz, DMSO-*d$_6$*) δ ppm 8.70 (s, 1 H), 7.47−7.29 (m, 4 H), 6.62 (d, *J* = 8.02 Hz, 1 H), 4.13 (t, *J* = 7.73 Hz, 1 H), 3.64 (s, 3 H), 2.21−2.10 (m, 1 H), 1.69−1.46 (m, 6 H), 1.36−1.23 (m, 2 H); ^{13}C NMR (126 MHz, DMSO-*d$_6$*) δ ppm 173.18 (1 C, C=O), 154.75 (1 C, C=O), 139.47 (1 C, ArC), 131.52 (2 C, ArCH), 119.54 (1 C, ArCH), 112.69 (1 C, ArC), 55.60 (1 C, CH), 51.82 (1 C, CH$_3$), 41.59 (1 C, CH), 28.63 (1 C, CH$_2$), 28.22 (1 C, CH$_2$), 24.89 (1 C, CH$_2$), 24.67 (1 C, CH$_2$).

Rac-methyl 2-[(4-bromophenyl)carbamoylamino]-2-cyclohexyl-acetate (36) Prepared according to procedure A with intermediate **33** (3 mmol) and methyl 2-amino-2-cyclohexyl-acetate (1.1 equiv., 3.3 mmol). Crude product was dry loaded on silica and purified by flash column chromatography (silica gel, PE/EA 10−>60%, gradient). The beige solid was washed with diethyl ether (15 mL), filtered and dried under high vacuum. Yield: 682 mg, 70%; Appearance: white solid; LCMS: 1.87 min, *m/z* 369.1, 371.1 ((M+H)$^+$ 1:1, $^{79/81}$Br), Method B; ^{1}H NMR (500 MHz, DMSO-*d$_6$*) δ ppm 8.67 (s, 1 H), 7.40−7.28 (m, 4 H), 6.57 (d, *J* = 8.59 Hz, 1 H), 4.12 (dd, *J* = 8.59, 5.73 Hz, 1 H), 3.62 (s, 3 H), 1.73−1.63 (m, 3 H), 1.58−1.52 (m, 2 H), 1.25−0.96 (m, 6 H); ^{13}C NMR (126 MHz, DMSO-*d$_6$*) δ ppm 172.67 (1 C, C=O), 154.68 (1 C, C=O), 139.49 (1 C, ArC), 131.48 (2 C, ArCH), 119.44 (2 C, ArCH), 112.60 (1 C, ArC), 57.10 (1 C, NCH), 51.79 (1 C, CH$_3$), 29.16 (1 C, CH), 28.57 (1 C, CH$_2$), 27.95 (1 C, CH$_2$), 25.64 (1 C, CH$_2$), 25.49 (2 C, CH$_2$).

Rac-methyl 2-[(4-bromophenyl)carbamoylamino]-3-cyclohexyl-propanoate (37) Prepared according to procedure A with intermediate **33** (3 mmol) and methyl 2-amino-3-cyclohexyl-propanoate HCl (1 equiv. 3.3 mmol). Crude product was dry loaded on silica and purified by flash column chromatography (silica gel, PE/EA 10−>60%, gradient). The beige solid was washed with diethyl ether (15 mL), filtered, and dried under high vacuum to afford desired product as a white solid. Yield: 410 mg, 40%; Appearance: white solid; LCMS: 1.97 min, *m/z* 383.2, 385.1 ((M+H)$^+$ 1:1, $^{79/81}$Br), Purity 90%, Method B; ^{1}H NMR (500 MHz, DMSO-*d$_6$*) δ ppm 8.68 (s, 1 H), 7.39−7.30 (m, 4 H), 6.57 (d, *J* = 8.02 Hz, 1 H), 4.22 (td, *J* = 8.31, 5.73 Hz, 1 H), 3.61 (s, 3 H), 1.70 (br. d, *J* = 12.60 Hz, 1 H), 1.66−1.54 (m, 5 H), 1.50 (ddd, *J* = 8.74, 5.58, 3.44 Hz, 2 H), 1.22−1.03 (m, 4 H), 0.96−0.79 (m, 2 H); ^{13}C NMR (126 MHz, DMSO-*d$_6$*) δ ppm 173.86 (1 C, C=O), 154.66 (1 C, C=O), 139.50 (1 C, ArC), 131.43 (2 C, ArCH), 119.57 (2 C, ArCH), 112.63 (1 C, ArC), 51.88 (1 C, CH$_3$), 50.14 (1 C, CH), 33.53 (1 C, CH$_2$), 33.07 (1 C, CH$_2$), 31.70 (1 C, CH), 25.96 (1 C, CH$_2$), 25.76 (1 C, CH$_2$), 25.57 (1 C, CH$_2$).

Rac-methyl 2-[(4-bromophenyl)carbamoylamino]-2-tetrahydropyran-4-yl-acetate (38) Prepared according to procedure A with intermediate **33** (3 mmol) and methyl 2-amino-2-tetrahydropyran-4-yl-acetate **56** (3 mmol). Crude product was purified via FCC (PE/EA 0−>70%) then additionally washed with diethyl ether to remove impurities from aliphatic region. Yield: 510 mg, 70%; Appearance: white solid; LCMS: 1.93 min, *m/z* 371.1, 373.0 ((M+H)$^+$ 1:1, $^{79/81}$Br), Method B; ^{1}H NMR (500 MHz, CHLOROFORM-*d*) δ ppm 7.43−7.37 (m, 2 H) 7.25−7.19 (m, 2 H) 6.92 (s, 1 H) 5.61 (d, *J* = 8.59 Hz, 1 H) 4.57 (dd, *J* = 8.59, 5.16 Hz, 1 H) 3.78 (s, 3 H) 4.04−3.95 (m, 2 H) 3.44−3.32 (m, 2 H) 2.13−2.03 (m, 1 H) 1.61−1.42 (m, 4 H); ^{13}C NMR (126 MHz, DMSO-*d$_6$*) δ ppm 172.29 (1 C, C=O), 154.68 (1 C, C=O), 139.42 (1 C, ArC), 131.48 (2 C, ArCH), 119.52 (2 C, ArCH), 112.70 (1 C, ArC), 66.62 (2 C, CH$_2$), 56.57 (1 C, CH$_3$), 51.91 (1 C, CH), 37.22 (1 C, CH), 29.03 (1 C, CH$_2$), 27.99 (1 C, CH$_2$).

Tert-Butyl (2S)-2-[(4-bromophenyl)carbamoylamino]-4-methyl-pentanoate (39) Prepared according to procedure A with **33** (2.7 mmol) and H-Leu-OtBu HCl (1.1 equiv., 3 mmol); Crude product was dry loaded onto silica and purified by flash column chromatography (EA/PE 1:1 gradient). Yield: 700 mg, 70%;

Appearance: white solid; LCMS: 2.00 min, *m/z* 329.9, 331.9 ((M+H)$^+$ 1:1, $^{79/81}$Br, without tert-butyl group); Purity>95%, Method D; ^{1}H NMR (500 MHz, CHLOROFORM-*d*) δ ppm 7.33−7.28 (m, 2 H), 7.24−7.20 (m, 2 H), 7.11 (s, 1 H), 5.86 (d, *J* = 8.02 Hz, 1 H), 4.43 (ddd, *J* = 9.74, 8.02, 5.16 Hz, 1 H), 1.81−1.72 (m, 1 H), 1.67−1.59 (m, 1 H), 1.52 (s, 9 H), 1.50−1.43 (m, 1 H), 0.97 (dd, *J* = 6.59, 4.87 Hz, 6 H); ^{13}C NMR (126 MHz, DMSO-*d*$_6$) δ ppm 172.53 (1C, C=O), 154.62 (1 C, C=O), 139.57 (1C, ArC.), 131.44 (2C, ArCH), 119.54 (2C, ArCH), 112.57 (ArCBr), 80.61 (1C, C(CH$_3$)$_3$), 51.39 (CH), 40.85 (1C, CH$_2$), 27.65 (3C, C(CH$_3$)$_3$), 24.41 (1C, CH), 22.69 (1C, CH$_3$), 21.67 (1C, CH$_3$); Data corresponded to that reported in the literature [49].

General ester hydrolysis procedure B1:

A solution of ester in formic acid was stirred at room temperature for 3 h. The resulting mixture was quenched with water then extracted with ethyl acetate. Crude product was purified by flash column chromatography (PE/EtOAc) to obtain desired product as white solid.

2-[(4-bromophenyl)carbamoylamino]acetic acid (41) Prepared according to procedure B1 with intermediate tert-butyl 2-[(4-bromophenyl) carbamoylamino]acetate (34). Crude product was dry loaded onto silica and purified by flash column chromatography (silica gel, PE/EtOAc 6/4). Yield: 460 mg, 80%; Appearance: white solid; LCMS: 1.09 min, *m/z* 273.1, 275.1 ((M+H)$^+$ 1:1, $^{79/81}$Br), Purity >95%, Method B; ^{1}H NMR (500 MHz, DMSO-*d*$_6$) δ ppm 12.56 (br. s, 1 H), 8.90 (s, 1 H), 7.39−7.27 (m, 4 H), 6.37 (t, *J* = 5.73 Hz, 1 H), 3.75 (d, *J* = 5.73 Hz, 2 H); ^{13}C NMR (126 MHz, DMSO-*d*$_6$) δ ppm 172.13 (1 C, C=O), 155.01 (1 C, C=O), 139.78 (1 C, ArC), 131.43 (2 C, ArCH), 119.57 (2 C, ArCH), 112.51 (1 C, ArC), 41.33 (1 C, CH$_2$).

General ester hydrolysis procedure B2: Methyl 2-[(4-bromophenyl)carbamoylamino]-2-tetrahydropyran-4-yl-acetate (1 eq.) was suspended in the mixture methanol (3 mL)/water (2 mL) and 2M solution of sodium hydroxide (1 mL) was added. RM was stirred for 2 h at room temperature. Methanol was evaporated, the remaining solution was acidified with 1M HCl (pH = 2−3). The precipitation was filtered washed with water and dried to give final product as a white powder.

2-[(4-bromophenyl)carbamoylamino]-2-cyclopentyl-acetic acid (42) Prepared according to procedure B2 with intermediate Methyl 2-[(4-bromophenyl)carbamoylamino]-2-cyclopentyl-acetate (35). Yield: 479 mg, 79%; Appearance: white solid; LCMS: 1.55 min, *m/z* 341.1, 343.1 ((M+H)$^+$ 1:1, $^{79/81}$Br), Purity = 90%, Method D; ^{1}H NMR (500 MHz, DMSO-*d*$_6$) δ ppm 9.03 (s,1 H), 7.37 (m, 4 H), 6.65 (d, *J* = 8.02 Hz, 1 H), 4.06 (dd, *J* = 8.02, 6.30 Hz, 1 H), 2.26−2.16 (m, 1 H), 1.68−1.27 (m, 8 H); . ^{13}C NMR (126 MHz, DMSO-*d*$_6$) δ ppm 174.40 (1 C, C=O), 154.98 (1 C, C=O), 140.15 (1 C, ArC), 131.30 (2 C, ArCH), 119.34 (2 C, ArCH), 112.02 (1 C, ArC), 55.74 (1 C, CH), 42.20 (1 C, CH), 28.76 (s, 1 C, CH$_2$), 27.72 (1 C, CH$_2$), 24.80 (2 C, CH$_2$).

2-[(4-bromophenyl)carbamoylamino]-2-cyclohexyl-acetic acid (43) Prepared according to procedure B2 with intermediate methyl 2-[(4-bromophenyl)carbamoylamino]-2-cyclohexyl-acetate (36). The crude product was not purified further and was taken for next step. Yield: 480 mg, 97%; Appearance: white solid; LCMS: 1.04 min, *m/z* 355, 357 ((M+H)$^+$ 1:1, $^{79/81}$Br), Purity>90%, Method B; ^{1}H NMR (500 MHz, DMSO-*d*$_6$) δ ppm 12.69 (br. s, 1 H), 8.72 (s, 1 H), 7.40−7.30 (m, 4 H), 6.43 (d, *J* = 8.59 Hz, 1 H), 4.07 (dd, *J* = 8.59, 4.58 Hz, 1 H), 1.75−1.48 (m, 6 H), 1.27−1.13 (m, 2 H), 1.13−0.96 (m, 3 H); ^{13}C NMR (126 MHz, DMSO-*d*$_6$) δ ppm 173.60 (1 C, C=O), 154.76 (1 C, C=O), 139.65 (1 C, ArC), 131.55 (2 C, ArCH), 119.42 (2 C, ArCH), 112.46 (1 C, ArC), 56.91 (1 C, NCH), 29.31 (1 C, CH), 27.67 (2 C, CH$_2$), 25.64 (3 C, CH$_2$).

2-[(4-bromophenyl)carbamoylamino]-3-cyclohexyl-propanoic acid (44) Prepared according to procedure B2 with intermediate methyl 2-[(4-bromophenyl)carbamoylamino]-3-cyclohexyl-propanoate (37). The crude product was not purified further and was taken for next step. Yield: 200 mg, 60%;

Appearance: white solid; LCMS: 1.16 min, *m/z* 369.1, 371.1 ((M+H)$^+$ 1:1, $^{79/81}$Br), Purity>95%, Method B; ^{1}H NMR (500 MHz, DMSO-*d*$_6$) δ ppm 8.93 (s, 1 H), 7.34 (m, 4 H), 6.57 (br d, *J* = 8.02 Hz, 1 H), 4.11 (td, *J* = 8.59, 5.16 Hz, 1 H), 1.73 (br d, *J* = 12.03 Hz, 1 H), 1.61 (m, 3 H), 1.59−1.41 (m, 3 H), 1.34 (br d, *J* = 2.86 Hz, 1 H), 1.20−1.04 (m, 3 H), 0.96−0.77 (m, 2 H); ^{13}C NMR (126 MHz, DMSO-*d*$_6$) δ ppm 174.96 (1 C, C=O), 154.72 (1 C, C=O), 139.79 (1 C, ArC), 131.41 (2 C, ArCH), 119.41 (2 C, ArCH), 112.34 (1 C, ArC), 50.35 (1 C, CH), 39.51 (1 C, CHCH$_2$), 33.63 (1 C, CH$_2$), 33.19 (1 C, CH$_2$), 31.91 (1 C, CH), 26.02 (1 C, CH$_2$), 25.80 (1 C, CH$_2$), 25.65 (1 C, CH$_2$); once carbon (CHCH$_2$) hidden under DMSO peak.

2-[(4-bromophenyl)carbamoylamino]-2-tetrahydropyran-4-yl-acetic acid (45) Prepared according to procedure B2 with intermediate methyl 2-[(4-bromophenyl)carbamoylamino]-2-tetrahydropyran-4-yl-acetate (38). The crude product was used for next reaction without further purification. Yield: 286 mg, 90%; Appearance: white solid; LCMS: 1.36 min, *m/z* 357.1, 359.1 ((M+H)$^+$ 1:1, $^{79/81}$Br), Purity>95%, Method D; ^{1}H NMR (500 MHz, DMSO-*d*$_6$) δ ppm 12.83 (br. s, 1 H), 7.40−7.34 (m, 4 H), 6.62 (d, *J* = 8.59 Hz, 1 H), 4.13 (dd, *J* = 8.59, 5.16 Hz, 1 H), 3.89−3.83 (m, 2 H), 3.27 (qd, *J* = 11.74, 2.00 Hz, 2 H), 2.01−1.93 (m, 1 H), 1.51−1.29 (m, 4 H); ^{13}C NMR (126 MHz, DMSO-*d*$_6$) δ ppm 173.19 (1 C, C=O), 154.80 (1 C, C=O), 139.65 (1 C, ArC), 131.70 (2 C, ArCH), 119.45 (2 C, ArCH), 112.48 (1 C, ArC), 66.78 (2 C, CH$_2$), 56.40 (1 C, CH), 37.30 (1 C, CH), 29.21 (1 C, CH$_2$), 27.83 (1 C, CH$_2$).

(2S)-2-[(4-bromophenyl)carbamoylamino]-4-methyl-pentanoic acid (46) Prepared according to procedure B1 with intermediate tert-butyl (2S)-2-[(4-bromophenyl)carbamoylamino]-4-methyl-pentanoate (39) (2 mmol). Crude product was purified by flash column chromatography (silica gel, PE/EtOAc 2/8, gradient). Yield: 440 mg, 83% Appearance: white solid; LCMS: 0.90 min, *m/z* 329.0, 331.0 ((M+H)$^+$ 1:1, $^{79/81}$Br), Purity>95%, Method B; ^{1}H NMR (500 MHz, DMSO-*d*$_6$) δ ppm 12.66 (s, 1 H), 8.71 (s, 1 H), 7.43−7.32 (m, 4 H), 6.45 (d, *J* = 8.59 Hz, 1 H), 4.17 (td, *J* = 8.59, 5.73 Hz, 1 H), 1.67 (dquin, *J* = 13.75, 6.73 Hz, 1 H), 1.57−1.46 (m, 2 H), 0.90 (dd, *J* = 10.31, 6.30 Hz, 6 H); Data corresponded to that reported in the literature [49].

1-[(4-bromophenyl)carbamoylamino]cyclo-pentanecarboxylic acid (47) 1-bromo-4-isocyanato-benzene (0.76 mmol) was dissolved in dichloromethane (10 mL) at room temperature and methyl 1-aminocyclopentanecarboxylate HCl (0.76 mmol, 1.0 equiv.) was added in one portion. Then triethylamine (1.15 mmol, 1.5 equiv.) was added to the solution and RM was stirred at room temperature overnight. The RM was diluted with DCM and washed twice with water. Organic layer was passed through the phase separator and concentrated under reduced pressure. The intermediate 40 was used directly in the next step. A 2-(4-bromoanilino)-3-oxa-1-azaspiro[4.4]non-1-en-4-one (0.42 mmol) was suspended in the mixture methanol (2 mL)/water (3 mL) and 2M solution of sodium hydroxide (0.847 mmol, 0.424 mL) was added. RM was stirred for 4 h at room temperature. Methanol was evaporated, the remaining solution was acidified with 1M HCl (pH = 2−3). The precipitation was filtered washed with water and dried to give final product as a white powder. Yield: 119 mg, 85%; LCMS:1.35 min, *m/z* 327.1, 329.1 ((M+H)$^+$ 1:1, $^{79/81}$Br), Purity> 95%, Method C; ^{1}H NMR (500 MHz, DMSO-*d*$_6$) δ ppm 8.56 (s, 1 H), 7.39−7.31 (m, 4 H), 6.59 (s, 1 H), 2.11−2.03 (m, 2 H), 1.89−1.82 (m, 2 H), 1.70−1.66 (m, 4 H); ^{13}C NMR (126 MHz, DMSO-*d*$_6$) δ ppm 176.52 (1 C, C=O), 155.05 (1 C, C=O), 140.26 (1 C, ArC.), 131.88 (2 C, ArCH), 119.87 (2 C, ArCH), 112.82 (1 C, ArC.), 65.30 (1 C, Cgem.), 37.35 (2 C, CH$_2$), 24.61 (2 C, CH$_2$).

General procedure C for amide coupling using T3P: SM was dissolved in ethyl acetate, then amine (1 equiv), TEA, (1.5 equiv.), and T3P (1.5 equiv.) were added. Reaction mixture was stirred overnight at room temperature, then EtOAc was added and washed

with water. An organic layer was dried over Na_2SO_4, filtered, and concentrated under reduced pressure. Crude product was purified by reverse phase flash column chromatography.

2-[(4-bromophenyl)carbamoylamino]-N-(3-pyridyl)acetamide (6) Prepared according to procedure C with intermediate 2-[(4-bromophenyl) carbamoyl amino]acetic acid (**41**) (1 equiv., 0.15 mmol) and 3-aminopyridine (1.1 equiv., 0.17 mmol). Yield: 40 mg, 80%; Appearance: white solid; LCMS:1.21 min, *m/z* 349.2, 351.1 ((M+H)+ 1:1, [79/81]Br), Purity> 95%, Method B; ^{1}H NMR (500 MHz, DMSO-*d*$_6$) δ ppm 10.28 (br. s., 1 H), 9.02 (s, 1 H), 8.74 (d, *J* = 2.86 Hz, 1 H), 8.26 (dd, *J* = 4.87, 1.43 Hz, 1 H), 8.03 (dq, *J* = 8.16, 1.48 Hz, 1 H), 7.41−7.38 (m, 4 H), 7.38−7.34 (m, 1 H), 6.52 (t, *J* = 5.44 Hz, 1 H), 3.96 (d, *J* = 5.73 Hz, 2 H); ^{13}C NMR (126 MHz, DMSO-*d*$_6$) δ ppm 169.13 (1 C, C=O), 155.09 (1 C, C=O), 144.26 (1 C, ArCH), 140.77 (1 C, ArCH), 139.77 (1 C, ArC), 135.54 (1 C, ArC), 131.42 (2 C, ArCH), 126.06 (1 C, ArCH), 123.68 (1 C, ArCH), 119.50 (2 C, ArCH), 112.49 (1 C, ArC), 43.20 (1 C, CH$_2$); HRMS: Exact Mass: 348.0222; (M+H)+: 349.0300; Mass Observed: 349.0292; 2.33 ppm.

(2S)-2-[(4-bromophenyl)carbamoylamino]-4-methyl-N-(3-pyridyl)pentanamide (7) Prepared according to procedure C with intermediate tert-butyl (2S)-2-[(4-bromophenyl)carbamoylamino]-4-methyl-pentanoic acid (**46**) (0.14 mmol) and 3-aminopyridine (1.3 equiv., 0.18 mmol). Yield: 34 mg, 61%; Appearance: white solid; LCMS: 1.54 min, *m/z* 405.2, 407.1 ((M+H)+ 1:1, [79/81]Br), Purity>95%, method B; ^{1}H NMR (500 MHz, DMSO-*d*$_6$) δ ppm 10.38 (s, 1 H), 8.77−8.69 (m, 2 H), 8.24 (dd, *J* = 4.87, 1.43 Hz, 1 H), 8.02 (dq, *J* = 8.16, 1.48 Hz, 1 H), 7.40−7.27 (m, 5 H), 6.52 (d, *J* = 8.02 Hz, 1 H), 4.49−4.33 (m, 1 H), 1.73−1.59 (m, 1 H), 1.56−1.44 (m, 2 H), 0.91 (d, *J* = 6.30 Hz, 6 H); ^{13}C NMR (126 MHz, DMSO-*d*$_6$) δ ppm 172.46 (1 C, C=O), 154.64 (1 C, C=O), 144.41 (1 C, ArCH), 140.94 (1 C, ArCH), 139.60 (1 C ArC), 135.56 (1 C, ArC), 131.47 (2 C, ArCH), 126.30 (1 C, ArCH), 123.69 (1 C, ArCH), 119.48 (2 C, ArCH), 112.55 (1 C, ArC), 52.09 (1 C, CH), 41.76 (1 C, CH$_2$), 24.43 (1 C, CH), 23.05 (1 C, CH$_3$), 21.82 (1 C, CH$_3$); HRMS: Exact Mass: 404.0848; (M+H)+: 405.0926; Observed Mass: 405.0921; 1.27 ppm.

2-[(4-bromophenyl)carbamoylamino]-2-cyclopentyl-N-(3-pyridyl)acetamide (8) Prepared according to procedure C with intermediate 2-[(4-bromophenyl)carbamoylamino]-2-cyclopentyl-acetic acid (**42**) (0.11 mmol) and 3-aminopyridine (1.1 equiv., 0.122 mmol). Crude product was purified by reverse phase column chromatography (C18 12 g, Water pH-10/MeOH 90/10 → 100) to give final product. Yield: 22 mg, 47%; Appearance: white solid; LCMS: 1.57 min *m/z* 417.2, 419.1 ((M+H)+ 1:1, [79/81]Br), Purity>95% method B; ^{1}H NMR (500 MHz, DMSO-*d*$_6$) δ ppm 10.44 (s, 1 H), 8.80 (s, 1 H), 8.77 (d, *J* = 1.72 Hz, 1 H), 8.27 (dd, *J* = 4.58, 1.15 Hz, 1 H), 8.07−8.03 (m, 1 H), 7.41−7.31 (m, 5 H), 6.61 (d, *J* = 8.59 Hz, 1 H), 4.33 (t, *J* = 8.02 Hz, 1 H), 2.20 (sxt, *J* = 7.90 Hz, 1 H), 1.72−1.55 (m, 4 H), 1.54−1.45 (m, 2 H), 1.43−1.31 (m, 2 H); ^{13}C NMR (126 MHz, DMSO-*d*$_6$) δ ppm 171.80 (1 C, C=O), 154.76 (1 C, C=O), 144.39 (1 C, ArCH), 140.92 (1 C, ArCH), 139.62 (1 C, ArC), 135.50 (1 C, ArC), 131.53 (2 C, ArCH), 126.24 (1 C, ArCH), 123.77 (1 C, ArCH), 119.46 (2 C, ArCH), 112.53 (1 C, ArC), 56.57 (1C, CH), 42.73 (1 C, CH), 28.65 (1 C, CH$_2$), 28.22 (1 C, CH$_2$), 24.85 (1 C, CH$_2$), 24.67 (1 C, CH$_2$); HRMS: Exact Mass: 416.0848; (M+H)+: 417.0926; Observed Mass: 417.0922; 0.99 ppm.

2-[(4-bromophenyl)carbamoylamino]-N-(3-pyridyl)-2-tetrahydropyran-4-yl-acetamide (9) Prepared according to procedure C with intermediate 2-[(4-bromophenyl)carbamoylamino]-2-tetrahydropyran-4-yl-acetic acid (**43**) (0.14 mmol) and 3-aminopyridine (1.1 equiv., 0.16 mmol). Crude product was purified by reverse phase column chromatography (C18 12 g, Water pH-10/MeOH 90/10−>100) to give final product. Yield: 25 mg, 41%; Appearance: white solid; LCMS: 1.99 min, *m/z* 433.1, 435.1 ((M+H)+ 1:1, [79/81]Br), Purity>95%, Method D; ^{1}H NMR (500 MHz, DMSO-*d*$_6$)

δ ppm 10.51 (s, 1 H), 8.87 (s, 1 H), 8.77 (d, *J* = 3.44 Hz, 1 H), 8.28 (dd, *J* = 4.58, 1.72 Hz, 1 H), 8.10−8.02 (m, 1 H), 7.41−7.34 (m, 5 H), 6.69 (br d, *J* = 8.59 Hz, 1 H), 4.35 (dd, *J* = 8.59, 6.87 Hz, 1 H), 3.91−3.82 (m, 2 H), 3.31−3.22 (m, 2 H), 1.98−1.88 (m, 1 H), 1.57 (br d, *J* = 11.46 Hz, 1 H), 1.48−1.40 (m, 2 H), 1.30 (qd, *J* = 12.51, 4.30 Hz, 1 H); ^{13}C NMR (126 MHz, DMSO-*d*$_6$) δ ppm 170.77 (1 C, C=O), 154.76 (1 C, C=O), 144.26 (1 C, ArCH), 140.89 (1 C, ArCH), 139.60 (1 C, ArC), 135.30 (1 C, ArC), 131.43 (2 C, ArCH), 126.35 (1 C, ArCH), 123.86 (1 C, ArCH), 119.41 (2 C, ArCH), 112.54 (1 C, ArC), 66.59 (2 C, CH$_2$), 57.48 (1 C, CH), 38.14 (1 C, CH), 29.21 (1 C, CH$_2$), 28.30 (1 C, CH$_2$); HRMS: Exact Mass: 432.0797; (M+H)+: 433.0877; Observed Mass: 433.0879; 0.46 ppm.

2-[(4-bromophenyl)carbamoylamino]-3-cyclohexyl-N-(3-pyridyl)propenamide (10) Prepared according to procedure C with intermediate 2-[(4-bromophenyl)carbamoylamino]-3-cyclohexyl-propanoic acid (**44**) (0.087 mmol) and 3-aminopyridine (1.1 equiv., 0.1 mmol). Crude product was purified by reverse phase column chromatography (C18 12 g, Water pH-10/MeOH 90/10−>100) to give final product. Yield: 8 mg, 21%; Appearance: white solid; LCMS: 2.31min, *m/z* 445.2, 457.2 ((M+H)+ 1:1, [79/81]Br), Purity>95%, Method D; ^{1}H NMR (500 MHz, CHLOROFORM-*d*) δ ppm 9.91 (br. s, 1 H), 8.72 (d, *J* = 2.29 Hz, 1 H), 8.31 (dd, *J* = 4.58, 1.15 Hz, 1 H), 7.88−7.82 (m, 1 H), 7.80 (br s, 1 H), 7.19 (d, *J* = 9.17 Hz, 2 H), 7.11 (dd, *J* = 8.31, 4.87 Hz, 1 H), 6.94 (d, *J* = 9.17 Hz, 2 H), 6.77 (br d, *J* = 7.45 Hz, 1 H), 4.84−4.74 (m, 1 H), 1.81−1.51 (m, 8 H), 1.43 (br s, 1 H), 1.21−0.84 (m, 4 H); HRMS: Exact Mass: 444.1161; (M+H)+: 445.1239; Observed Mass: 445.1234; 1.15 ppm.

2-[(4-bromophenyl)carbamoylamino]-2-cyclopentyl-N-pyrimidin-5-yl-acetamide (13) Prepared according to procedure C with intermediate 2-[(4-bromophenyl)carbamoylamino]-2-cyclopentyl-acetic acid (**42**) (0.15 mmol) and pyrimidin-5-amine (1.2 equiv., 0.18 mmol). The crude product was purified by flash column chromatography (silica gel, PE/EA 10−>100%, then EA/MeOH 2% gradient). Yield: 29 mg, 65%; Appearance: white solid; LCMS: 2.15 min, *m/z* 418.1, 420.1 ((M+H)+ 1:1, [79/81]Br), Purity>95%, Method D; ^{1}H NMR (500 MHz, DMSO-*d*$_6$) δ ppm 10.66 (s, 1 H), 9.02 (s, 2 H), 8.90 (s, 1 H), 8.79 (s, 1 H), 7.40−7.34 (m, 4H), 6.64 (d, *J* = 8.59 Hz, 1 H), 4.33 (t, *J* = 8.02 Hz, 1 H), 2.21 (sxt, *J* = 8.60 Hz, 1 H), 1.75−1.57 (m, 4 H), 1.57−1.47 (m, 2 H), 1.46−1.28 (m, 2 H); ^{13}C NMR (126 MHz, DMSO-*d*$_6$) δ ppm 172.22 (1 C, C=O), 154.76 (1 C, C=O), 153.28 (1 C, ArCH), 147.21 (2 C, ArCH), 139.54 (1 C, ArC), 134.17 (1 C, ArC), 131.61 (2 C, ArCH), 119.47 (2 C, ArCH) 112.59 (1 C, ArC.), 56.57 (1 C, CH), 42.48 (1 C, CH), 28.69 (1 C, CH$_2$), 28.19 (1 C, CH$_2$), 24.65 (2 C, CH$_2$); HRMS: Exact mass: 417.0800; (M+H)+: 418.0880; Observed mass: 418.0877; 0.81 ppm.

Tert-butyl 3-[[2-[(4-bromophenyl)carbamoylamino]-2-cyclopentyl-acetyl]amino] azetidine-1-carboxylate (48) was prepared according to procedure C with intermediate 2-[(4-bromophenyl)carbamoylamino]-2-cyclopentyl-acetic acid (**42**) (0.11 mmol) and tert-butyl 3-aminoazetidine-1-carboxylate (1.1 equiv., 0.122 mmol). Crude product was purified by reverse phase column chromatography (C18 12 g, Water pH-10/MeOH 90/10 → 100) to give final product. Yield: 27 mg, 49%; Appearance: white solid; LCMS: 1.76 min, *m/z* 495.1, 497.1 ((M+H)+ 1:1, [79/81]Br), Purity>90%, Method B; ^{1}H NMR (500 MHz, DMSO-*d*$_6$) δ ppm 8.74 (s, 1 H), 8.73 (s, 1 H), 7.40−7.27 (m, 4 H), 6.41 (d, *J* = 8.59 Hz, 1 H), 4.41−4.33 (m, 1 H), 4.09−3.95 (m, 2 H), 3.72−3.57 (m, 2 H), 2.12−1.99 (m, 1 H), 1.63−1.41 (m, 6 H), 1.35 (s, 9 H), 1.32−1.23 (m, 2 H); ^{13}C NMR (126 MHz, DMSO-*d*$_6$) δ ppm 172.40 (s, 1 C, C=O), 156.00 (1 C, C=O), 155.13 (s, 1 C, C=O), 140.25 (1 C, ArC), 132.01 (2 C, ArCH), 119.91 (2 C, ArCH), 112.91 (1 C, ArC), 79.22 (1 C, C(CH$_3$)$_3$), 56.21 (1 C, CH), 43.36 (1 C, CH), 39.13 (2 C, CH$_2$), 29.17 (1 C, CH), 28.59 (3 C, C(CH$_3$)$_3$), 28.55 (2 C, CH$_2$), 25.26 (2 C, CH$_2$).

General procedure D for BOC deprotection: Starting material was dissolved in dichloromethane and hydrochloric acid (4 mol/l)

in 1,4-dioxane (5−10 equiv.) was added. Reaction mixture was stirred at room temperature for 2.5 h. The solvent was evaporated, and crude product was purified by preparative HPLC (19 × 100mm (5 μm) C-18 Waters Xbridge, MeOH, pH = 10) to obtain final product.

N-(azetidin-3-yl)-2-[(4-bromophenyl)carbamoylamino]-2-cyclopentyl-acetamide (14) Prepared according to procedure D with intermediate tert-butyl 3-[[2-[(4-bromophenyl)carbamoylamino]-2-cyclopentyl-acetyl]amino] azetidine-1-carboxylate (48). The crude product was purified by preparative HPLC (19 × 100mm (5 μm) C-18 Waters Xbridge, MeOH, pH = 10); Yield: 10 mg, 27%; Appearance: white solid; LCMS: 2.05 min, m/z 395.1, 397.1 ((M+H)$^+$ 1:1, $^{79/81}$Br), Purity>90%, Method D;^{1}H NMR (500 MHz, DMSO-d_6) δ ppm 8.82 (s, 1 H), 8.62 (d, J = 6.87 Hz, 1 H), 7.40−7.31 (m, 4 H), 6.45 (d, J = 9.17 Hz, 1 H), 4.44 (sxt, J = 7.33 Hz, 1 H), 4.10 (t, J = 8.31 Hz, 1 H), 3.51 (t, J = 7.45 Hz, 2 H), 3.39 (t, J = 7.73 Hz, 2 H), 2.05 (qd, J = 7.80, 15.54 Hz, 1 H), 1.61−1.43 (m, 6 H), 1.37−1.24 (m, 2 H); HRMS: Exact Mass: 394.1004; (M+H)$^+$: 395.1083; Observed Mass: 395.1078; 1.17 ppm.

2-[(4-bromophenyl)carbamoylamino]-2-cyclopentyl-N-(1-methyl-4-piperidyl) acetamide (15) Prepared according to procedure C with intermediate 2-[(4-bromophenyl)carbamoylamino]-2-cyclopentyl-acetic acid (42) (0.11 mmol) and 4-amino-1-methylpiperidine (1.1 equiv., 0.122 mmol). The crude product was purified by preparative flash column chromatography (19 × 100mm (5 μm) C-18 Waters Xbridge, MeOH, pH = 10). Yield: 5 mg, 10%; Appearance: white solid; LCMS: 2.17 min, m/z 437.1, 439.1 ((M+H)$^+$ 1:1, $^{79/81}$Br), Purity>95%, Method D; ^{1}H NMR (500 MHz, DMSO-d_6) δ ppm 8.78 (s, 1 H), 8.24 (br d, J = 7.45 Hz, 1 H), 7.41−7.31 (m, 4 H), 6.44 (d, J = 9.17 Hz, 1 H), 4.10 (br t, J = 8.02 Hz, 1 H), 2.89 (br s, 2 H), 3.75 (br. s, 1 H), 2.12−2.01 (m, 2 H), 2.73−2.55 (m, 3 H), 1.95−1.82 (m, 2 H), 1.46 (s, 1 H), 1.64−1.43 (m, 8 H), 1.38−1.22 (m, 2H); two protons are hidden under DMSO peak; HRMS: Exact Mass: 436.1474; (M+H)$^+$: 437.1552; Observed Mass: 437.1549; 0.72 ppm.

2-[(4-bromophenyl)carbamoylamino]-2-cyclopentyl-N-(oxetan-3-yl)acetamide (16) Prepared according to procedure C with intermediate 2-[(4-bromophenyl)carbamoylamino]-2-cyclopentyl-acetic acid (42) (0.11 mmol) and 3-oxetanamine (1.1 equiv., 0.122 mmol). The crude product was purified by preparative flash column chromatography (19 × 100mm (5 μm) C-18 Waters Xbridge, MeOH, pH = 10); Yield: 2.6 mg, 6%; Appearance: white solid; LCMS: 1.41 min, m/z 396.1, 398.1 ((M+H)$^+$ 1:1, $^{79/81}$Br), Purity>95%, Method B; ^{1}H NMR (500 MHz, DMSO-d_6) δ ppm 8.90 (d, J = 6.30 Hz, 1 H), 8.77 (s, 1 H), 7.44−7.29 (m, 4 H), 6.43 (d, J = 8.59 Hz, 1 H), 4.82−4.73 (m, 1 H), 4.70 (td, J = 6.73, 2.00 Hz, 2 H), 4.47−4.34 (m, 2 H), 4.15−4.15 (m, 1 H), 2.07 (sxt, J = 7.90 Hz, 1 H), 1.64−1.42 (m, 6 H), 1.39−1.24 (m, 2 H); HRMS: Exact Mass: 395.0845; (M+H)$^+$: 396.0923; Observed Mass: 396.0918; 1.21 ppm.

2-[(4-bromophenyl)carbamoylamino]-2-cyclopentyl-N-tetrahydropyran-4-yl-acetamide (17): Prepared according to procedure C with intermediate 2-[(4-bromophenyl)carbamoylamino]-2-cyclopentyl-acetic acid (42) (0.11 mmol) and 4-aminotetrahydropyran (1.1 equiv., 0.122 mmol). Crude product was purified by reverse phase column chromatography (C18 12 g, Water pH-10/MeOH 90/10 → 100) to give final product. Yield: 22 mg, 47%; Appearance: white solid; LCMS: 2.13 min m/z 424.2, 426.2 ((M+H)$^+$ 1:1, $^{79/81}$Br), Purity>95% method D;^{1}H NMR (500 MHz, DMSO-d_6) δ ppm 8.76 (s, 1 H), 8.11 (d, J = 8.02 Hz, 1 H), 7.40−7.27 (m, 4H), 6.38 (d, J = 9.17 Hz, 1 H), 4.13−4.05 (m, 1 H), 3.83−3.68 (m, 3 H), 2.02 (sxt, J = 8.02 Hz, 1 H), 1.63 (d, J = 12.60 Hz, 2 H), 1.59−1.47 (m, 4 H), 1.46−1.23 (m, 6 H); ^{13}C NMR (126 MHz, DMSO-d_6) δ ppm 170.95 (1 C. C=O), 154.56 (1 C, C=O), 139.81 (1 C, ArC), 131.49 (1 C, ArCH), 119.41 (1 C, ArCH), 112.32 (1 C, ArC), 65.86 (2 C, CH$_2$), 55.46 (1 C, CH), 44.77 (1 C, CH), 43.41 (1 C, CH), 32.52

(2 C, CH$_2$), 28.58 (2 C, CH$_2$), 24.87 (1 C, CH$_2$), 24.64 (1 C, CH$_2$); HRMS: Exact Mass: 423.1158; (M+H)$^+$: 424.1236; Observed Mass: 424.1231; 1.13 ppm.

2-[(4-bromophenyl)carbamoylamino]-2-cyclopentyl-N-(tetrahydrofuran-2-ylmethyl)acetamide (18) Prepared according to procedure C with intermediate 2-[(4-bromophenyl)carbamoylamino]-2-cyclopentyl-acetic acid (42) (0.11 mmol) and 3-oxetanamine (1.1 equiv., 0.122 mmol). Crude product was purified by reverse phase column chromatography (C18 12 g, Water pH-10/MeOH 90/10 → 100) to give final product. Yield: 31 mg, 62%; Appearance: white solid; LCMS: 2.26 min, m/z 424.2, 426.2 ((M+H)$^+$ 1:1, $^{79/81}$Br), Purity>95%, Method D; ^{1}H NMR (500 MHz, DMSO-d_6) δ ppm 8.79 (s, 1 H), 8.22−8.14 (m, 1 H), 7.42−7.30 (m, 4 H), 6.41 (d, J = 9.17 Hz, 1 H), 4.16 (ddd, J = 8.74, 7.30, 2.86 Hz, 1 H), 3.85−3.78 (m, 1 H), 3.77−3.69 (m, 1 H), 3.63−3.56 (m, 1 H), 3.25−3.14 (m, 1 H), 3.11−3.03 (m, 1 H), 2.08 (sxt, J = 7.79 Hz, 1 H), 1.89−1.71 (m, 3 H), 1.62−1.40 (m, 7 H), 1.39−1.24 (m, 2 H); ^{13}C NMR (126 MHz, DMSO-d_6) δ ppm 172.01 (1 C, C=O), 154.58 (1 C, C=O), 139.82 (1 C, ArC.), 131.43 (2 C, ArCH), 119.30 (2 C, ArCH), 112.30 (1 C, ArC), 76.96 (1 C, CH), 67.19 (1 C, CH$_2$), 55.48 (1 C, CH), 43.09 (1 C, CH), 42.58 (1 C, CH$_2$), 28.57 (1 C, CH$_2$), 28.43 (1 C, CH$_2$), 27.99 (1 C, CH$_2$), 25.14 (1 C, CH$_2$), 24.86 (1 C, CH$_2$), 24.69 (1 C, CH$_2$); HRMS: Exact Mass: 423.1158; (M+H)$^+$: 424.1236; Observed Mass: 424.1234; 0.42 ppm.

2-[(4-bromophenyl)carbamoylamino]-2-cyclopentyl-N-(1,3-dimethylpyrazol-4-yl)acetamide (19): Prepared according to procedure C with intermediate 2-[(4-bromophenyl)carbamoylamino]-2-cyclopentyl-acetic acid (42) (0.11 mmol) and 1,3-dimethyl-1h-pyrazol-4-amine (1.1 equiv., 0.122 mmol). Crude product was washed with diethyl ether to give products. Yield: 48 mg, 99%; Appearance: beige solid; LCMS: 2.14 min, m/z 434.1, 436.1 ((M+H)$^+$ 1:1, $^{79/81}$Br), Purity>95%, Method D; ^{1}H NMR (500 MHz, DMSO-d_6) δ ppm 9.51 (s, 1 H), 8.81 (s, 1 H), 7.45−7.43 (m, 1 H), 7.41−7.33 (m, 4 H), 6.52−6.48 (m, 1 H), 4.35 (t, J = 8.31 Hz, 1 H), 3.68 (s, 3 H), 2.19−2.11 (m, 4 H), 1.65−1.53 (m, 4 H), 1.53−1.32 (m, 4 H); ^{13}C NMR (126 MHz, DMSO-d_6) δ ppm 171.11 (1 C, C=O), 155.20 (1 C, C=O), 140.29 (1 C, ArC.), 132.89 (1 C, ArC), 132.06 (1C, ArC), 130.63 (2 C, ArCH), 119.95 (2 C, ArCH), 118.21 (1 C, ArCH), 112.90 (1 C, ArC), 56.03 (1 C, CH), 43.71 (1 C, CH), 36.92 (1 C, CH$_3$), 29.17 (1 C, CH$_2$), 28.70 (1 C, CH$_2$), 25.23 (2 C, CH$_2$), 9.32 (1 C, CH$_3$); HRMS: Exact Mass: 433.1113; (M+H)$^+$: 434.1193; Observed Mass: 434.1187; 1.39 ppm.

2-[(4-bromophenyl)carbamoylamino]-2-cyclopentyl-N-(1-isopropylpyrazol-4-yl)acetamide (20): Prepared according to procedure C with intermediate 2-[(4-bromophenyl)carbamoylamino]-2-cyclopentyl-acetic acid (42) (0.11 mmol) and 1-isopropyl-1h-pyrazol-4-amine (1.1 equiv., 0.122 mmol). Crude product was washed with diethyl ether to give products. Yield: 50 mg, 100%; Appearance: white solid; LCMS: 2.23 min, m/z 448.1, 450.1 ((M+H)$^+$ 1:1, $^{79/81}$Br), Purity>95%, Method D; ^{1}H NMR (500 MHz, DMSO-d_6) δ ppm 10.18 (s, 1 H) 8.78 (s, 1 H), 7.88 (s, 1 H), 7.42 (s, 1 H), 7.40−7.33 (m, 4 H), 6.50 (d, J = 8.59 Hz, 1 H), 4.43 (dt, J = 13.32, 6.80 Hz, 1 H), 4.19 (t, J = 8.02 Hz, 1 H), 2.14 (sxt, J = 7.90 Hz, 1 H), 1.69−1.53 (m, 4 H), 1.53−1.43 (m, 2 H), 1.37 (d, J = 6.87 Hz, 6 H), 1.35−1.29 (m, 2 H); ^{13}C NMR (126 MHz, DMSO-d_6) δ ppm 169.31 (1 C, C=O), 154.69 (1 C, C=O), 139.68 (1 C, ArC), 131.54 (2 C, ArCH), 129.36 (1 C, ArCH), 120.77 (1 C, ArC), 119.43 (2 C, ArCH), 118.12 (1 C, ArCH), 112.42 (1 C, ArC), 56.10 (1 C, CH), 52.94 (1 C, CH), 42.73 (1 C, CH), 28.66 (1 C, CH$_2$), 28.30 (1 C, CH$_2$), 24.66 (2 C, CH$_2$), 22.63 (1 C, CH$_3$); HRMS: Exact Mass: 447.127; (M+H)$^+$:448.135; Observed Mass: 448.1345; 1.12 ppm.

2-[(4-bromophenyl)carbamoylamino]-2-cyclopentyl-N-pyridazin-3-yl-acetamide (21) Prepared according to procedure C with intermediate 2-[(4-bromophenyl)carbamoylamino]-2-cyclopentyl-acetic acid (42) (0.11 mmol) and 3-aminopyridazine

(1.1 equiv., 0.122 mmol). Crude product was washed with diethyl ether to give products. Yield: 14.3 mg, 31%; Appearance: white solid; LCMS: 2.07 min, *m/z* 418.1, 420.1 ((M+H)$^+$ 1:1, $^{79/81}$Br), Purity>95%, Method D; ^{1}H NMR (500 MHz, DMSO-*d*$_6$) δ ppm 11.31−11.20 (br.s, 1 H), 8.94 (dd, *J* = 4.58, 1.72 Hz, 1 H), 8.79 (s, 1 H), 8.27 (dd, *J* = 9.17, 1.72 Hz, 1 H), 7.65 (dd, *J* = 9.17, 4.58 Hz, 1 H), 7.33 (q, *J* = 9.17 Hz, 4 H), 6.56 (d, *J* = 8.02 Hz, 1 H), 4.46 (t, *J* = 7.73 Hz, 1 H), 2.19 (sxt, *J* = 7.79 Hz, 1 H), 1.73−1.53 (m, 4 H), 1.52−1.38 (m, 3 H), 1.35−1.25 (m, 1 H); ^{13}C NMR (126 MHz, DMSO-*d*$_6$) δ ppm 173.17 (1 C, C=O), 155.39 (1 C, ArC), 154.77 (1 C, C=O), 148.62 (1 C, ArCH), 139.60 (1 C, ArC), 131.50 (2 C, ArCH), 128.56 (1 C, ArCH), 119.51 (2 C, ArCH), 118.38 (1 C, ArCH), 112.53 (1 C, ArC), 56.49 (1 C, CH), 42.33 (1 C, CH), 28.55 (1 C, CH$_2$), 28.13 (1 C, CH$_2$), 24.68 (2 C, CH$_2$);; HRMS: Exact Mass: 417.0800; (M+H)$^+$ 418.0880; Observed Mass: 418.0876; 0.96 ppm.

1-[(4-bromophenyl)carbamoylamino]-N-(3-pyridyl)cyclopentanecarboxamide (22) Prepared according to procedure C with intermediate 1-[(4-bromophenyl)carbamoylamino]cyclopentanecarboxylic acid (**47**) (0.21 mmol) and 3-aminopyridine (1.1 equiv., 0.23 mmol). Crude product was dry loaded on silica and purified by flash column chromatography (silica gel, PE/EA 10−>100%, EA/MeOH 2% gradient).; Yield: 45 mg, 50%; Appearance: white solid; LCMS: 1.99 min, *m/z* 403.1, 405.1 (M+H)$^+$ (1:1, $^{79/81}$Br), Purity>95%, Method D; ^{1}H NMR (500 MHz, DMSO-*d*$_6$) δ ppm 9.75 (s, 1 H), 8.75 (d, *J* = 2.29 Hz, 1 H), 8.74−8.71 (m, 1 H), 8.23 (dd, *J* = 4.58, 1.72 Hz, 1 H), 8.06−7.99 (m, 1 H), 7.40−7.29 (m, 5 H), 6.54 (s, 1 H), 2.23−2.13 (m, 2 H), 1.91−1.82 (m, 2 H), 1.75−1.67(m, 4 H); ^{13}C NMR (126 MHz, DMSO-*d*$_6$) d ppm 173.40 (1 C, C=O), 154.20 (1 C, C=O), 143.99 (1 C, ArCH), 141.77 (1 C, ArCH), 139.52 (1 C, ArC), 136.00 (1 C, ArC, 131.61 (2 C, ArCH), 126.99 (1 C, ArCH), 123.51 (1 C, ArCH), 119.54 (2 C, ArCH), 112.53 (1 C, ArC), 66.49 (1 C, Cgem), 36.38 (1 C, CH$_2$), 36.29 (1 C, CH$_2$), 23.69 (2 C, CH$_2$); HRMS: Exact mass: 402.0691; (M+H)$^+$: 403.0771; Observed mass: 403.0760; 2.83 ppm.

1-[(4-bromophenyl)carbamoylamino]-N-pyrimidin-5-yl-cyclopentanecarboxamide (23) Prepared according to procedure C with intermediate 1-[(4-bromophenyl)carbamoylamino]cyclopentanecarboxylic acid (**47**) (0.21 mmol) and 5-aminopyrimidine (1.1 equiv., 0.23 mmol). Crude product was dry loaded on silica and purified by flash column chromatography (silica gel, PE/EA 10−>100%, EA/MeOH 2% gradient).; Yield: 37 mg, 43%; Appearance: white solid; LCMS: 2.03 min, *m/z* 404.1, 406.1 ((M+H)$^+$ 1:1, $^{79/81}$Br), Purity>95%, Method D; ^{1}H NMR (500 MHz, DMSO-*d*$_6$) δ ppm 9.97 (s, 1 H), 9.03 (s, 2 H), 8.85 (s, 1 H), 8.70 (s, 1 H), 7.40−7.31 (m, 4 H), 6.60 (s, 1 H), 2.24−2.14 (m, 2 H), 1.90−1.80 (m, 2 H), 1.76−1.68 (m, 4 H); ^{13}C NMR (126 MHz, DMSO-*d*$_6$) δ ppm 173.85 (1 C, C=O), 154.20 (1 C, C=O), 152.91 (1 C, ArCH), 147.83 (1 C, ArCH), 139.43 (1 C, ArC), 134.72 (1 C, ArC), 131.64 (2 C, ArCH), 119.58 (2 C, ArCH), 112.61 (1 C, ArC), 66.39 (1 C, Cgem), 36.41 (2 C, CH$_2$), 23.70 (2 C, CH$_2$); HRMS: Exact mass: 403.0644; (M+H)$^+$: 404.0724; Observed mass: 404.0723; 0.22 ppm.

1-[(4-bromophenyl)carbamoylamino]-N-(1,3-dimethylpyrazol-4-yl) cyclopentane carboxamide (24) Prepared according to procedure C with intermediate 1-[(4-bromophenyl) carbamoylamino] cyclopentane carboxylic acid (**47**) (0.14 mmol) and 1,3-dimethyl-1H-pyrazol-4-amine (1.1 equiv., 0.16 mmol). Crude product was purified by reverse phase column chromatography (C18 12 g, Water pH-10/MeOH 90/10 → 100) to give final product. Yield: 20 mg, 43%; Appearance: white solid; LCMS: 1.92 min, *m/z* 420.1, 422.1 (M+H$^+$ 1:1, $^{79/81}$Br), Purity>95%, Method D; ^{1}H NMR (500 MHz, DMSO-*d*$_6$) δ ppm 8.96 (s, 1 H), 8.70 (s, 1 H), 7.41−7.33 (m, 4 H), 7.24 (s, 1 H), 6.52 (s, 1 H,), 3.66 (s, 3 H), 2.18−2.09 (m, 2 H), 2.06 (s, 3 H), 1.90−1.82 (m, 2 H), 1.71−1.65 (m, 4 H); ^{13}C NMR (126 MHz, DMSO-*d*$_6$) δ ppm 172.91 (1 C, C=O), 154.28 (1 C, C=O), 139.73 (1 C, ArC), 133.32 (1 C, ArC), 131.89 (1 C, ArCH), 131.45 (2 C, ArCH), 119.35 (2 C, ArCH), 117.82 (1 C, ArC), 112.38 (1 C, ArC),

66.13 (1 C, Cgem), 36.49 (2 C, CH$_2$), 36.37 (1 C, CH$_3$), 23.72 (2 C, CH$_2$), 8.82 (1 C, CH$_3$); HRMS: Exact Mass: 419.0957; (M+H)$^+$: 420.1037; Observed Mass: 420.1030; 1.67 ppm.

1-[(4-bromophenyl)carbamoylamino]-N-(2H-tetrazol-5-ylmethyl) cyclopentanecarboxamide (25): Prepared according to procedure C with intermediate 1-[(4-bromophenyl)carbamoylamino] cyclopentane carboxylic acid (**47**) (0.14 mmol) and c-(2h-tetrazol-5-yl)-methylamine (1.1 equiv., 0.16 mmol). Crude product was purified by reverse phase column chromatography (C18 12 g, Water pH-10/MeOH 90/10 → 100) to give final product. Yield: 20 mg, 40%; Appearance: white solid; LCMS: 1.55 min, *m/z* 408.1, 410.1 ((M+H)$^+$ 1:1, $^{79/81}$Br), Purity>90%, Method D; ^{1}H NMR (500 MHz, DMSO-*d*$_6$) δ ppm 8.78 (br s, 1 H), 8.54 (br s, 1 H), 7.49−7.28 (m, 4 H), 6.74 (br s, 1 H), 4.54 (br d, *J* = 5.16 Hz, 2 H), 2.08 (br d, *J* = 13.17 Hz, 2 H), 1.66 (br s, 4 H) 1.81 (br d, *J* = 12.60 Hz, 2 H); ^{13}C NMR (126 MHz, DMSO-*d*$_6$) δ ppm 174.74 (1 C, C=O), 154.99 (1 C, C=O), 154.84 (1 C, ArC), 139.40 (1 C, ArC), 131.46 (2 C, ArCH), 119.62 (2 C, ArCH), 112.73 (1 C, ArC), 65.86 (1 C, Cgem), 36.52 (2 C, CH$_2$), 33.18 (1 C, CH$_2$), 23.79 (2 C, CH$_2$);; HRMS: Exact Mass: 407.0705; (M+H)$^+$: 408.0785; Observed Mass: 408.0777; 1.97 ppm.

1-[(4-bromophenyl)carbamoylamino]-N-(1-methyl-4-piperidyl) cyclopentane carboxamide (26): Prepared according to procedure C with intermediate 1-[(4-bromophenyl)carbamoylamino] cyclopentane carboxylic acid (**47**) (0.12 mmol) and 4-amino-1-methylpiperidine (1.1 equiv., 0.13 mmol). The crude product was purified by preparative flash column chromatography (19 × 100mm (5 μm) C-18 Waters Xbridge, MeOH, pH = 10); Yield: 10 mg, 20%; Appearance: white solid; LCMS: 2.00 min, *m/z* 423.1, 425.1 ((M+H)$^+$ 1:1, $^{79/81}$Br), Purity>90%, Method D; ^{1}H NMR (500 MHz, DMSO-*d*$_6$) δ 8.68 (s, 1H), 7.40−7.31 (m, 4H), 6.41 (s, 1 H), 3.59−3.48 (m, 1H), 2.75 (d, *J* = 9.16 Hz, 2 H), 2.21 (s, 3 H), 2.14 (d, *J* = 12.03 Hz, 2 H), 2.07−1.97 (m, 2H), 1.83−1.74 (m, 2 H), 1.64 (m, 6 H), 1.40−1.51 (m, 2 H); ^{13}C NMR (126 MHz, DMSO-*d*$_6$) δ ppm 173.33 (1C, C=O) 154.20 (1 C, C=O) 139.78 (1 C, ArC) 131.40 (2 C, ArCH) 119.37 (2 C, ArCH) 112.29 (1 C, ArC) 65.98 (1 C, Cgem) 53.81 (2 C, CH$_2$) 48.61 (1 C, CH) 45.29 (1 C, CH$_3$) 36.39 (2 C, CH$_2$) 30.72 (2 C, CH$_2$) 23.75 (2 C, CH$_2$); HRMS: Exact Mass: 422.1317; (M+H)$^+$ 423.1397; Observed Mass: 423.1390; 1.66 ppm.

1-[(4-bromophenyl)carbamoylamino]-N-(1-isopropylpyrazol-4-yl) cyclopentane carboxamide (27) Prepared according to procedure C with intermediate 1-[(4-bromophenyl) carbamoylamino] cyclopentanecarboxylic acid (**47**) (0.12 mmol) and 1-isopropyl-1h-pyrazol-4-amine (1.1 equiv., 0.13 mmol). Crude product was washed with diethyl ether to obtain desired product.; Yield: 36 mg, 68%; Appearance: white solid; LCMS: 2.01 min, *m/z* 434.1, 436.1 (M+H$^+$ 1:1, $^{79/81}$Br), Purity>95%, Method D; ^{1}H NMR (500 MHz, DMSO-*d*$_6$) δ ppm 9.61 (s, 1 H) 8.62 (s, 1 H), 7.86 (s, 1 H), 7.42 (d, *J* = 1.15 Hz, 1 H), 7.36−7.28 (m, 4 H), 6.43 (s, 1 H), 4.38 (quin, *J* = 6.73 Hz, 1 H), 2.13−2.04 (m, 2 H), 1.82−1.76 (m, 2 H), 1.69−1.62 (m, 4 H), 1.33 (d, *J* = 6.87 Hz, 6 H); ^{13}C NMR (126 MHz, DMSO-*d*$_6$) δ ppm 171.30 (1 C, C=O), 154.08 (1 C, C=O), 139.66 (1 C, ArC), 131.45 (2 C, ArCH), 129.39 (1 C, ArCH), 121.71 (1 C, ArC), 119.29 (2 C, ArCH), 117.90 (1 C, ArCH), 112.38 (1 C, ArC), 66.04 (1 C, Cgem), 52.84 (1 C, CH), 36.56 (2 C, CH$_2$), 23.74 (2 C, CH$_2$), 22.67 (2 C, CH$_3$); HRMS: Exact Mass: 433.1113; Observed Mass: 434.1187; 1.39 ppm.

1-[(4-bromophenyl)carbamoylamino]-N-(2-pyridyl)cyclopentanecarboxamide (28) Prepared according to procedure C with intermediate 1-[(4-bromophenyl)carbamoylamino] cyclopentane carboxylic acid (**47**) (0.12 mmol) and 2-aminopyridine (1.1 equiv., 0.13 mmol). The crude product was purified by preparative flash column chromatography (19 × 100mm (5 μm) C-18 Waters Xbridge, MeOH, pH = 10); Yield: 3.8 mg, 7.7%; Appearance: white solid; LCMS: 2.08 min, *m/z* 403.1, 405.1 ((M+H)$^+$ 1:1, $^{79/81}$Br), Purity>95%, Method D; ^{1}H NMR (500 MHz, DMSO-*d*$_6$) δ 9.85 (s, 1H), 8.91 (s, 1H), 8.22 (d, *J* = 4.81 Hz, 1H), 8.06 (d, *J* = 8.17 Hz, 1H),

7.77−7.72 (m, 1H), 7.39−7.27 (m, 4H), 7.09−6.98 (m, 1H), 6.65 (s, 1H), 2.19−2.10 (m, 2H), 1.93−1.85 (m, 2H), 1.69−1.63 (m, 4H); HRMS: Exact Mass: 402.0691; $(M+H)^+$ 403.0771; Observed Mass: 403.0769; 0.5 ppm.

1-[(4-bromophenyl)carbamoylamino]-N-(6-methyl-3-pyridyl) cyclopentane carboxamide (29) Prepared according to procedure C with intermediate 1-[(4-bromophenyl)carbamoylamino] cyclopentane carboxylic acid (**47**) (0.12 mmol) and 5-amino-2-methylpyridine (1.1 equiv., 0.13 mmol). The crude product was purified by preparative flash column chromatography (19 × 100mm (5 μm) C-18 Waters Xbridge, MeOH, pH = 10). Yield: 15 mg, 29%; Appearance: white solid; LCMS: 2.05 min, m/z 417.1, 419.1 $((M+H)^+$ 1:1, $^{79/81}$Br), Purity>95%, Method D; ^{1}H NMR (500 MHz, DMSO-d_6) δ 9.67 (s, 1H), 8.78 (s, 1H), 8.60 (d, $J = 2.86$ Hz, 1H), 7.89 (dd, $J = 2.58$, 8.31 Hz, 1H), 7.40−7.31 (m, 4H), 7.16 (d, $J = 8.02$ Hz, 1H), 6.59 (s, 1H), 2.39 (s, 3H), 2.20−2.12 (m, 2H), 1.89−1.82 (m, 2H), 1.70 (t, $J = 6.87$ Hz, 4H); ^{13}C NMR (126 MHz, DMSO-d_6) δ ppm 173.24 (1 C, C=O), 154.22 (1 C, C=O), 152.09 (1 C, ArC.), 140.94 (1 C, ArCH), 139.59 (1 C, ArC), 133.50 (1 C, ArC), 131.46 (2 C, ArCH), 127.66 (1 C, ArCH), 122.50 (1 C, ArCH), 119.39 (2 C, ArCH), 112.46 (1 C, ArC), 66.47 (1 C, Cgem), 36.35 (2 C, CH$_2$), 23.70 (2 C, CH$_2$), 23.33 (1 C, CH$_3$); HRMS: Exact Mass: 416.0848; $(M+H)^+$:417.0928; Observed Mass: 417.0924; 0.96 ppm.

1-[(4-bromophenyl)carbamoylamino]-N-(5-methyl-3-pyridyl) cyclopentane carboxamide (30): Prepared according to procedure C with intermediate 1-[(4-bromophenyl)carbamoylamino] cyclopentane carboxylic acid (**47**) (0.12 mmol) and 3-amino-5-methylpyridine (1.1 equiv., 0.13 mmol). The crude product was purified by preparative flash column chromatography (19 × 100mm (5 μm) C-18 Waters Xbridge, MeOH, pH = 10); Yield: 10 mg, 20%; Appearance: white solid; LCMS: 2.10 min, m/z 417.1, 419.1 $((M+H)^+$ 1:1, $^{79/81}$Br), Purity = 88%, Method D; ^{1}H NMR (500 MHz, DMSO-d_6) δ ppm 9.66 (s, 1 H), 8.73 (s, 1 H), 8.55 (d, $J = 2.29$ Hz, 1 H), 8.05 (d, $J = 1.15$ Hz, 1 H), 7.84 (t, $J = 2.00$ Hz, 1 H), 7.39−7.26 (m, 4 H), 6.54 (s, 1 H), 2.23 (s, 3 H), 2.19−2.09 (m, 2 H), 1.87−1.78 (m, 2 H), 1.72−1.63 (m, 4 H); ^{13}C NMR (126 MHz, DMSO-d_6) δ ppm 173.37 (1 C, C=O) 154.20 (1 C, C=O) 144.22 (1 C, ArCH) 139.56 (1 C, ArC) 138.75 (1C., ArCH) 135.65 (1 C, ArC) 132.65 (1 C, ArCH) 131.47 (2 C, ArCH) 127.34 (1 C, ArC) 119.37 (2 C, ArCH) 112.49 (1 C, ArC) 66.49 (1 C, Cgem.) 36.33 (2 C, CH$_2$) 23.69 (2 C, CH$_2$) 17.87 (1 C, CH$_3$);; HRMS: Exact Mass: 416.0848; $(M+H)^+$: 417.0928; Observed Mass: 417.0925; 0.72 ppm.

1-[(4-bromophenyl)carbamoylamino]-N-(6-chloro-3-pyridyl) cyclopentane carboxamide (31): Prepared according to procedure C with intermediate 1-[(4-bromophenyl)carbamoylamino] cyclopentane carboxylic acid (**47**) (0.12 mmol) and 5-amino-2-chloropyridine (1.1 equiv., 0.13 mmol). Crude product was washed with diethyl ether to obtain desired product. Yield: 40 mg, 75%; Appearance: white solid; LCMS: 2.15 min, m/z 437.0, 439.0, 441.0 $((M+H)^+$ 3:4:2, $^{79/81}$Br and $^{35/37}$Cl), Purity>95%, Method D; ^{1}H NMR (500 MHz, DMSO-d_6) δ ppm 9.87 (s, 1 H), 8.69 (s, 1 H), 8.60 (d, $J = 2.29$ Hz, 1 H), 8.07 (dd, $J = 8.59$, 2.86 Hz, 1 H), 7.41 (d, $J = 8.59$ Hz, 1 H), 7.36−7.33 (m, 2 H), 7.31−7.28 (m, 2 H), 6.53 (s, 1 H), 2.19−2.10 (m, 2 H), 1.86−1.77 (m, 2 H), 1.71−1.64 (m, 4 H); ^{13}C NMR (126 MHz, DMSO-d_6) δ ppm 174.05 (1 C, C=O) 154.70 (1 C, C=O) 143.91 (1 C, ArC) 141.62 (1 C, ArCH) 139.98 (1 C, ArC) 136.20 (1 C, ArC) 131.94 (2 C, ArCH) 131.06 (1 C, ArCH) 124.50 (s, 1 C, ArCH) 120.02 (2 C, ArCH) 113.09 (1 C, ArC) 66.99 (1 C, Cgem) 36.86 (2 C, CH$_2$) 24.20 (2 C, CH$_2$); HRMS: Exact Mass: 436.0302; $(M+H)^+$: 437.0382 Observed Mass: 437.0374; 1.83 ppm.

(2S)-2-(tert-butoxycarbonylamino)-3-cyclopropyl-propanoic acid (49) The cyclohexylamine (CHA) salts need to be converted to the free acid before they can be utilized in carbodiimide coupling. Commercially available (2S)-2-(tert-butoxycarbonylamino)-3-cyclopropyl-propanoic acid CHA salt was dissolved in

dichloromethane (5 mL). The DCM solution was washed with ice-cold aqueous KHSO$_4$ solution 3 times. The organic layer filtered through a phase separator. The solvent was evaporated under reduced pressure to obtain the free acid. Yield: 50 mg, 80%; Appearance: colourless liquid; LCMS: UV inactive; ^{1}H NMR (500 MHz, CHLOROFORM-d) δ ppm 11.10 (br s, 1 H), 5.18 (br d, $J = 8.02$ Hz, 1 H), 4.58−4.30 (m,1 H), 1.80−1.60 (m, 2 H), 1.44 (s, 9 H), 0.89−0.67 (m, 1 H), 0.55−0.42 (m, 2 H), 0.21−0.04 (m, 2 H).

Tert-butyl N-[(1S)-1-(cyclopropylmethyl)-2-oxo-2-(3-pyridylamino)ethyl]carbamate (51) Prepared according to procedure C with intermediate **49** (0.19 mmol) and 3-aminopyridine (1.3 equiv.) The resulting product was purified by reverse phase column chromatography (C-18, ACN/water pH-10 10:90 → 80:20) to give desired product Yield: 30 mg, 35%; Appearance: white solid; LCMS: 1.30 min, m/z 306.3 $(M+H)^+$ Purity >90%, Method B; ^{1}H NMR (500 MHz, CHLOROFORM-d) δ ppm 9.03−8.81 (m, 1 H), 8.59 (d, $J = 2.29$ Hz, 1 H), 8.31 (br. s., 1 H), 8.06 (br. s., 1 H), 7.21 (br. s., 1 H), 5.38 (d, $J = 7.45$ Hz, 1 H), 4.39 (br. s., 1 H), 1.83−1.65 (m, 2 H), 1.47−1.45 (m, 9 H), 0.85−0.75 (m, 1 H), 0.56−0.46 (m, 2 H), 0.18−0.10 (m, 2 H).

(2S)-2-amino-3-cyclopropyl-N-(3-pyridyl)propenamide HCl (53) Prepared according to general procedure D with the intermediate tert-butyl N-[(1S)-1-(cyclopropylmethyl)-2-oxo-2-(3-pyridylamino)ethyl]carbamate (**51**) (0.13 mmol). The crude product was used in the next step without further purification. Yield: 30 mg, 95%; Appearance: white solid; LCMS: 0.26 min, m/z 206.2, $(M+H)^+$ Purity >90%, Method B; ^{1}H NMR (500 MHz, DMSO-d_6) δ ppm 9.07 (d, $J = 2.29$ Hz, 1 H), 8.53 (dd, $J = 5.16$, 1.15 Hz, 1 H), 8.50−8.45 (m, 3 H), 8.45−8.42 (m, 1H), 7.79 (dd, $J = 8.59$, 5.16 Hz, 1 H), 4.24−4.10 (m,1 H), 1.93−1.85 (m, 1 H), 1.71−1.61 (m, 1 H), 0.87−0.76 (m, 1 H), 0.47−0.34 (m, 2 H), 0.18−0.05 (m, 2 H).

2-amino-2-cyclopropyl-N-(3-pyridyl)acetamide HCl (54) Prepared according to general procedure D with the intermediate (**52**) (0.395 mmol). The crude product was used in the next step without further purification. Yield: 85 mg, 95%; Appearance: off-white solid; LCMS: 0.54 min, m/z 192.2 $(M+H)^+$ Purity 90%, Method B; ^{1}H NMR (500 MHz, DMSO-d_6) δ ppm 12.09 (br s, 1 H), 9.16 (d, $J = 2.29$ Hz, 1 H), 8.59−8.54 (m, 4 H), 7.86 (dd, $J = 8.31$, 5.44 Hz, 1 H), 3.51 (dq, $J = 9.88$, 5.11 Hz, 1H), 1.19−1.09 (m, 1H), 1.08−1.00 (m, 1H), 0.71−0.60 (m, 1H), 0.59−0.51 (m, 2H).

(2S)-2-[(4-bromophenyl) carbamoyl amino]-3-cyclopropyl-N-(3 pyridyl) propenamide (11) Compound was prepared according to procedure A with 1-bromo-4-isocyanato-benzene (0.1 mmol) and the intermediate (2S)-2-amino-3-cyclopropyl-N-(3-pyridyl) propenamide HCl (**53**) (1 equiv., 0.1 mmol). Crude product was purified by reverse phase column chromatography (C18, acetonitrile/water pH = 10 10/90 → 80/20). Yield: 27 mg, 66%; Appearance: white solid; LCMS: 1.45 min, m/z 403.1, 405.1 $((M+H)^+$ 1:1, $^{79/81}$Br), Purity >95%, Method B ^{1}H NMR (500 MHz, DMSO-d_6) δ ppm 10.40 (s, 1 H), 8.86 (s, 1 H), 8.76 (d, $J = 1.72$ Hz, 1 H), 8.27 (dd, $J = 4.87$, 1.43 Hz, 1 H), 8.04 (ddd, $J = 8.31$, 2.58, 1.15 Hz, 1 H), 7.43−7.31 (m, 5 H), 6.64 (d, $J = 8.02$ Hz, 1 H), 4.46 (q, $J = 7.45$ Hz, 1 H), 1.70 (dt, $J = 13.75$, 6.87 Hz, 1 H), 1.52 (ddd, $J = 13.75$, 7.45, 6.30 Hz, 1 H), 0.85−0.65 (m, 1 H), 0.46−0.36 (m, 2 H), 0.15−0.03 (m, 2 H); ^{13}C NMR (126 MHz, DMSO-d_6) δ ppm 171.85 (1 C, C=O), 154.56 (1 C, C=O), 144.37 (1 C, ArCH), 140.93 (1 C, ArCH), 139.66 (1 C, ArC), 135.55 (1 C, ArC), 131.45 (2 C, ArCH), 126.25 (1 C, ArCH), 123.70 (1 C, ArCH), 119.47 (2 C, ArCH), 112.50 (1 C, ArC), 54.05 (1 C, CH), 37.70 (1 C, CH$_2$), 7.36 (1 C, CH), 4.41 (1 C, CH$_2$), 4.13 (1 C, CH$_2$); HRMS: Exact Mass: 402.0691; $(M+H)^+$: 403.0770; Observed Mass: 403.0763; 1.65 ppm.

2-[(4-bromophenyl)carbamoylamino]-2-cyclopropyl-N-(3-pyridyl)acetamide (12) Compound was prepared according to procedure A with 1-bromo-4-isocyanato-benzene (0.32 mmol) and the intermediate 2-amino-2-cyclopropyl-N-(3-pyridyl)acetamide

HCl (**54**) (1.1 equiv. 0.35 mmol). Crude product was purified by reverse phase column chromatography (C18, acetonitrile/water pH = 10 10/90 → 80/20). Yield: 85 mg, 69%; Appearance: white solid; LCMS: 1.37 min, m/z 389.1, 391.1 ((M+H)$^+$ 1:1, $^{79/81}$Br), Purity >95%, Method B; ^{1}H NMR (500 MHz, DMSO-d_6) δ ppm 10.35 (s, 1 H), 8.84 (s, 1 H), 8.78 (d, J = 1.72 Hz, 1 H), 8.28 (dd, J = 4.58, 1.15 Hz, 1 H), 8.06 (ddd, J = 8.31, 2.58, 1.15 Hz, 1 H), 7.40−7.33 (m, 5 H), 6.70 (d, J = 8.02 Hz, 1 H), 3.89 (t, J = 7.73 Hz, 1 H), 1.16−1.09 (m, 1 H), 0.59−0.46 (m, 3 H), 0.38−0.34 (m, 1 H); ^{13}C NMR (126 MHz, DMSO-d_6) δ ppm 171.29 (1 C, C=O), 154.51 (1 C, C=O), 144.43 (1 C, ArC), 140.80 (1 C, ArC), 139.57 (1 C, ArC), 135.57 (1 C, ArC.), 131.47 (2 C, ArCH), 126.14 (1 C, ArCH), 123.74 (1 C, ArCH), 119.47 (2 C, ArCH), 112.56 (1 C, ArC), 56.59 (1 C, CH), 14.34 (1 C, CH), 2.98 (1 C, CH$_2$), 2.30 (1 C, CH$_2$); HRMS: Exact Mass: 388.0535; (M+H)$^+$: 389.0613; Observed Mass: 389.0608; 1.32 ppm.

Methyl 2-(benzyloxycarbonylamino)-2-tetrahydropyran-4-ylidene-acetate (55) To acetonitrile (10 mL) solution of methyl 2-(benzyloxycarbonylamino)-2-dimethoxyphosphoryl-acetate (1 eq., 2 g), 1,8-diazabicyclo[5.4.0]undec-7-ene (1 eq., 0.92 g) was added at room temperature and stirred for 30 min. Acetonitrile (5 mL) solution of tetrahydropyran-4-one (1 eq., 0.60 g) was added and stirred overnight at room temperature. Water and ethyl acetate were added to the reaction mixture, and the organic layer was separated. The organic layer was washed with 2M HCl solution, saturated brine, water. Then the organic phase was filtered through the phase separator and concentrated under reduced pressure. Crude product was purified via flash column silica (50 g silica, PE:EtOAc 100:0, 70:30, 30:70) to obtain desired product as a white solid. Yield: 800 mg, 40%; Appearance: white solid; LCMS: 1.42 min, m/z 306.2 (M+H)$^+$, Purity >95%, Method B ^{1}H NMR (500 MHz, CHLOROFORM-d) δ ppm 7.45−7.29 (m, 5 H), 6.02 (br s, 1 H), 5.15 (s, 2 H), 3.97−3.51 (m, 7 H), 2.94 (br s, 2 H), 2.43 (t, J = 5.44 Hz, 2 H); Data corresponded to that reported in the literature [63,64].

Methyl 2-amino-2-tetrahydropyran-4-yl-acetate (56) The benzyl deprotection reaction was performed in the H-Cube reactor (10% Pd/C CatCart®, full hydrogen mode, 50 °C, 1.0 mL/min, one cycle). The reaction mixture was concentrated under reduced pressure. It was used in the next step without purification. Methyl 2-amino-2-tetrahydropyran-4-yl-acetate was obtained with high yield as a colourless oil. Yield: 440 mg, 98%; Appearance: colourless oil; LCMS: non-UV active; ^{1}H NMR (500 MHz, CHLOROFORM-d) δ ppm 4.03−3.96 (m, 2 H), 3.73 (s, 3 H), 3.37 (td, J = 11.74, 1.72 Hz, 2 H), 3.29 (d, J = 6.30 Hz, 1 H), 1.85 (tdt, J = 2×11.89, 6.01, 2 × 3.72 Hz, 1 H), 1.63−1.40 (m, 6 H); Data corresponded to that reported in the literature [63,64].

4.3. General biological and ADMET procedures

PathHunter® CHO−K1 FPRL1 cells (DISCOVERx) were grown in the F-12 nutrient mixture (HAM) (21765-037, Gibco®) supplemented with 10% Fetal Bovine Serum (A3840401, Thermo Fisher Sci), Hygromycin B 800 μg/mL (10687-010, Thermo Fisher Sci), Geneticin 300 μg/mL (10131-027, Thermo Fisher Sci). The cells were incubated at 37 °C and passaged every 2−3 days, based on the doubling time of the cell line. The Accutase ® (AT104-500) was used as the cell detachment solution.

β-Arrestin Path Hunter® assay detection protocol To identify novel FPR2 agonists PathHunter® CHO−K1 FPRL1 cells (DISCOVERx) expressing complementing fragments of the β-galactosidase (β-gal) enzyme were used. One day before the assay, the cells were diluted to a concentration of 0.5x10^6/mL in DISCOVERx plating media (Assay CompleteTM Cell Plating 2 Reagent; 93−0563R2A). The cells were plated out 10 μL per well of 384 well plate (5,000 cells per well) and incubated 1 h at room temperature then overnight at 37 °C. 10 mM stock solutions of compounds were

serially diluted in assay buffer (PBS using a half log dilution protocol on a Biomek instrument (automated liquid handler). The compound addition to the assay plate was performed Biomek instrument. Cells were stimulated with compounds or for high controls with W-peptide (a control ligand sequence WKYMVm; concentration = 100 nM) for 150 min at 37 °C. Detection reagent (19 parts Assay buffer, 5 parts Emerald II and 1 part Galacton Star; Pathhunter detection kit (93-0001) DISCOVERx) was added 12 μL per well and incubated for 60 min in the dark at room temperature. Receptor activation was determined by chemiluminescence using a BMG Pherastar plate reader. Raw data were entered into GraphPad Prism 7.01 analysis software for data processing and visualisation.

Calcium mobilization assay protocol The increase in cytosolic Ca^{2+} was measured by the FLIPR® Tetra® High-Throughput Cellular Screening System. In the calcium mobilization assay FLIPR calcium 6 dye (Molecular Devices) was used. One day before the assay, the cells were diluted to a concentration of 0.5x10^6/mL in F-12 nutrient mixture (HAM) (21765-037, Gibco®) containing 10% Fetal Bovine Serum (A3840401, Thermo Fisher Sci) and plated out 40 μL per well of 384 well plate (20,000 cells per well) then incubated 1 h at RT and then overnight at 37 °C. On the assay day, media was removed from the cell plate and 20 μL of dye per well were added. The cell plate was incubated for 2 h at 37 °C and later for 30 min at RT in the dark. 10 mM stock solutions of compounds were serially diluted in assay buffer (HBSS 20 mM HEPES) using a half log dilution protocol on a Biomek instrument (automated liquid handler). In both assays W-peptide was used as a control compound (100 nM). The 5 μL compound addition was performed by the FLIPR® Tetra® High-Throughput Cellular Screening System. The calcium mobilization was measured for 240s (Read Mode: Exc. Wavelength 470−495 nm, Em. Wavelength 515−575 nm, Gain: 2000). Data are processed using ScreenWorks 4.0.0.30. Raw data were entered into GraphPad Prism 7.01 analysis software for data processing and visualisation.

Isolation of human neutrophils from venous blood Blood was collected from healthy donors in accordance with a protocol approved by the Ludwig Maximilian University of Munich. Neutrophils were isolated from the blood using Polymorphprep (Axi-Shield) following the manufacturer's instructions. Isolated neutrophils were washed and resuspended in HBSS buffer containing 20 mM HEPES, 0.25% BSA, Ca2+ pH 7.4 (0.5x106 cells/mL) and used on the day of the experiment.

Human neutrophil static adhesion assay A static adhesion assay was performed with the aim of examining the small molecule agonists anti-inflammatory and proresolving properties. The day before the assay, 96-well flat-bottomed plates were coated with 50 μL of cell adhesion molecules with the final concentration 1 μg/mL: P-selectin (13025-H02H-100; SinoBiological) and ICAM- 1 (10346-H03H-100; SinoBiological). The coated plates were kept at 4 °C overnight. The excess of solution was removed with a pipette and the surface was blocked with BSA 2% for 1 h at room temperature. Neutrophils, 120 μL of neutrophils (0.5x10^6 cells/mL) per well, were pre-incubated with 30 μL of the agonists in non-coated plate (final dilution 1:5). Cells were incubated 30 min 37 °C with gentle continuous rocking. The pre-incubated neutrophils were added to the assay plate, 125 μL of pre-incubated neutrophils per well. The reaction was incubated for 20 min at 37 °C. Non-adherent neutrophils were removed, and the fixation step was performed with PFA 4%. Cells were stained with DAPI (Molecular Probes) for 10 min and then washed gently with 200 μL PBS. Four pictures per well were taken with a Leica microscope (DMI8, software: LAS X. V.3.4.2.18368, autofocus, exposure 51−57 ms, gain: 1.5, DAPI). The image files were processed using an ImageJ (National Institutes of Health). Raw data were entered into GraphPad Prism 7.01 analysis software (GraphPad Software, San Diego, CA, USA) for data processing and visualisation. Each compound was tested in technical

triplicates.

Statistical data analysis GraphPad Prism 7.01 (GraphPad Software, San Diego, CA, USA) was used for statistical analysis of the data. For comparison of treatment groups with the control group and P- value determination, the one-way Anova analysis followed by Dunnett's multiple comparison test was used. All data were shown as means $\pm$ SEM. Differences were considered statistically significant for a $P < 0.05$. P value; ***$P < 0.001$; **$P < 0.01$; *$P < 0.05$, ns — nonsignificant.

PK studies. The pharmacokinetic studies were performed in male C57BL6 mice with intraperitoneal administration at 10 mg/kg. In total 12 mice were used: 9 received the compound and 3 mice for blank plasma collection for bioanalysis. Compound concentration in plasma was measured at eight time points over 24 h. Each mouse used in the study was bled thrice with sufficient time gap. Mice (n = 12) were treated with either the vehicle (DMSO (10%) + PEG400 (35%) + PG (25%) + water (30%)) or the clear solution of Compound 8 (10 mg/kg in vehicle).

Cell Health Assay. In order to measure a variety of parameters which leads to cell viability, cell death, cytotoxicity or cell proliferation, the cell health assay was performed. A human hepatocyte carcinoma cells (HepG2 cells EACC origin) were cultured a week before assay in Eagle's Minimum Essential Medium (EMEM) inc. NEAA (non-essential amino acids) with 10% Fetal Bovine Serum and 2 mM GlutaMAX. During cell plating 1% Penicillin/Streptomyocin was added to media. 2000 HepG2 cells per well were plated in 25 μL media of a 384 well plate and incubated at 37 °C overnight. The compounds were added from the serial dilution plates using Biomek robot (automated liquid handler). The assay plates were incubated at 37 °C for 72 h. Four live staining dyes were added on Biomek robot and plates were incubate 1 h at 37 °C. Cell measurements were imaged on the InCELL Analyzer 2000 using the following four wavelength channels for each of the four dyes: Hoechst (nuclei) - DAPI channel; Fluo-4 AM (cellular calcium) - Fluorescein isothiocyanate (FITC) channel; Tetramethylrhodamine, methyl ester (TMRM) (mitochondria) - Texas Red channel; TOTO-3 (dead nuclei) − Cy® 5 channel. Raw data were processed and visualized in Genedata Screener analysis software. The cell measurements were normalised as a percentage in contradiction of low control. Any cell parameter that deviates from 100% baseline shows a variation in cell phenotype and cytotoxicity after drug treatment.

Kinetic solubility measurements The kinetic solubility was measured by diluting a 4 μL of 10 mM DMSO stock solution of the compound into PBS buffer pH 7.4 in a filtration plate at a target concentration of 200 μM giving a final solution composition of 98:2 PBS:DMSO. For each compound, measurements were performed in triplicates with two standard compounds (Verapamil and Ketoconazole) on the same plate. The filtration plate was agitated at 500 rpm for 90 min and then filtered into V-bottom plate. The filtrate was sampled and diluted further with a DMSO:PBS mixture in a flat bottomed UV plate resulting with a final solution composition of PBS:DMSO 80:20. A serial dilution for each compound was then performed in flat bottomed plates in PBS:DMSO 80:20 with concentrations 200 μM, 100 μM, 50 μM, 25 μM, 12.5 μM and 6.75 μM. The UV absorbance was read across 230−400 nm at 1 nm intervals using a TECAN Safire II plate reader and a suitable UV wavelength chosen around the UV maximum of each compound. This was used to calculate the concentration in the filtrate for each compound, and hence amount remaining in solution after 90 min which is reported as the kinetic solubility.

LogD measurements LogD measurements were conducted using the shake flask method. Compound was diluted from 10 mM DMSO stock solution into an Eppendorf containing equal amounts of octanol and phosphate buffered saline (PBS) to give a final concentration of 100 μM. The tubes were shaken for 12 h, centrifuged at 10000 rpm for 10 min and samples taken from the octanol and PBS layers. The samples from both layers were analysed in triplicate by LC-MS/MS (Agilent Technologies G6410 series, triple quadrupole with MM-ESI ion source) using optimised multiple reaction monitoring (MRM) scans and a standard column gradient on an Acquity UPLC BEH C8 1.7 μm column, running acetonitrile and water with 0.05% Acetic Acid as the mobile phase. The ratios of areas of the peaks were used to calculate the LogD in accordance with the equation: LogD = Log10(Area-TL/Area BL).

Microsomal stability assay The human and mouse liver microsomes (MLM) were obtained from BD Biosciences. The compounds were pre-incubated at 37 °C for 5 min with the microsomes and the reaction was initiated by adding an equal volume of NADPH generating solution (BD Biosciences). The final compound concentration in the incubation is 1 μM, and the microsomal protein concentration is 0.2 mg/mL. A sample was taken at t = 0 and quenched with two times volume of ice-cold methanol containing an internal standard reference compound (Carbamazepine). The reaction was agitated at 37 °C for 30 min, when a further sample was taken and quenched in an identical fashion. The samples were centrifuged at 10000 rpm for 10 min and the supernatant taken for analysis in triplicate by LC-MS/MS (Agilent Technologies G6410 series, triple quadrupole with MM-ESI ion source) using optimised multiple reaction monitoring scans and a standard column gradient on an Acquity UPLC BEH C8 1.7 μm column (mobile phase: acetonitrile and water with 0.05% acetic). The % turnover was obtained by calculating the percentage difference of the peak areas, normalised to the internal standard, at t = 0 and t = 30. Verapamil was used as the standard compound.

Contributors

TC supervised the findings of this work and conceived the studies. OS conceived and designed the neutrophil studies. AM was involved in planning and supervised the work. MP is the Coordinator of the Marie Skłodowska-Curie ITN EVOluTION and was involved in supervision the work. MM performed *in silico* studies, designed and synthesized the compounds, performed and analysed the *in vitro* assays. MM performed and analysed the human neutrophil static assays and contributed to all the stages of the experimental work. AOG and MM designed the human neutrophil static adhesion assay. SM aided in interpreting the results. MM and TC prepared the first draft of the manuscript. All authors have given approval to the final version of the manuscript.

Declaration of competing interest

The authors declare the following financial interests/personal relationships which may be considered as potential competing interests: MP is shareholder of ResoTher Pharma which is developing FPR2 peptide-agonists for clinical application. MM, TC, OS, AM, AOG and SM declare that they have no known competing financial interests or personal relationships that could have appeared to influence the work reported in this paper.

Appendix A. Supplementary data

Supplementary data to this article can be found online at https://doi.org/10.1016/j.ejmech.2021.113194.

Abbreviations

ACN	Acetonitrile
ADME	Absorption, Distribution, Metabolism, Excretion
BOC	*tert*-Butyloxycarbonyl
BSA	Bovine Serum Albumin
CL$_{int}$	Intrinsic Clearance
CVDs	Cardiovascular Diseases
DAPI	4′,6-Diamidino-2-phenylindole
DCC	*N,N′*-Dicyclohexylcarbodiimide
DCM	Dichloromethane
DCE	Dichloroethane
DIPEA	*N,N*-Diisopropylethylamine
DMAP	4-Dimethylaminopyridine
DMF	*N,N*−Dimethylformamide
DMSO	Dimethyl Sulfoxide
EC$_{50}$	Half Maximal Effective Concentration
E$_{max}$	Efficacy
FPR2	Formyl Peptide Receptor 2
GLASS database	GPCR-Ligand Association database
GPCR	G-Protein-Coupled Receptors
HBSS	Hanks' Balanced Salt Solution
HEPES	4-(2-Hydroxyethyl)-1-Piperazineethanesulfonic Acid
HLM	Human Liver Microsomes
HPLC	High Performance Liquid Chromatography
HRMS	High Resolution Mass Spectrometry
ICAM	Intercellular Adhesion Molecule
Ks	Kinetic Solubility
LC-MS	Liquid Chromatography-Mass Spectroscopy
LogD	Logarithm of Distribution-Coefficient
MLM	Mouse Liver Microsomes
NA	No Activity
NMR	Nuclear Magnetic Resonance
ON	Overnight
PE	Petroleum Ether
PFA	Paraformaldehyde
PK	Pharmacokinetics
RoI	Resolution of Inflammation
ROC	Receiver Operating Characteristic
SAA	Serum Amyloid A
SAR	Structure-Activity Relationship
TEA	Triethylamine
TM	Template Model
T3P	Propylphosphonic Anhydride
THF	Tetrahydrofuran
VCAM	Vascular Cell Adhesion Molecule

References

[1] M. Perretti, X. Leroy, E.J. Bland, T. Montero-Melendez, Resolution pharmacology: opportunities for therapeutic innovation in inflammation, Trends Pharmacol. Sci. 36 (11) (2015) 737−755.

[2] B.E. Sansbury, M. Spite, Resolution of acute inflammation and the role of resolvins in immunity, thrombosis, and vascular biology, Circ. Res. 119 (1) (2016) 113−130.

[3] J.M. Schwab, N. Chiang, M. Arita, C.N. Serhan, Resolvin E1 and protectin D1 activate inflammation-resolution programmes, Nature 447 (7146) (2007) 869−874.

[4] M.A. Sugimoto, L.P. Sousa, V. Pinho, M. Perretti, M.M. Teixeira, Resolution of inflammation: what controls its onset? Front. Immunol. 7 (2016).

[5] S.C. Heo, Y.W. Kwon, I.H. Jang, G.O. Jeong, T.W. Lee, J.W. Yoon, H.J. Shin, H.C. Jeong, Y. Ahn, T.H. Ko, S.C. Lee, J. Han, J.H. Kim, Formyl peptide receptor 2 is involved in cardiac repair after myocardial infarction through mobilization of circulating angiogenic cells, Stem Cell. 35 (3) (2017) 654−665.

[6] C.X. Qin, L.T. May, R. Li, N. Cao, S. Rosli, M. Deo, A.E. Alexander, D. Horlock, J.E. Bourke, Y.H. Yang, A.G. Stewart, D.M. Kaye, X.-J. Du, P.M. Sexton, A. Christopoulos, X.-M. Gao, R.H. Ritchie, Small-molecule-biased formyl peptide receptor agonist compound 17b protects against myocardial ischaemia-reperfusion injury in mice, Nat. Commun. 8 (1) (2017), 14232.

[7] R.A. García, B.R. Ito, J.A. Lupisella, N.A. Carson, M.-Y. Hsu, G. Fernando, M. Heroux, M. Bouvier, E. Dierks, E.K. Kick, D.A. Gordon, J. Chen, G. Mintier, M. Carrier, S. St-Onge, H. Shah, J. Towne, M.S. Bucardo, X. Ma, C.S. Ryan, N.R. Wurtz, J. Ostrowski, F.J. Villarreal, Preservation of post-infarction cardiac structure and function via long-term oral formyl peptide receptor agonist treatment, J. Am. Coll. Cardiol. Basic Trans. Science 349 (2019).

[8] S.D. Kim, S. Kwon, S.K. Lee, M. Kook, H.Y. Lee, K.-D. Song, H.-K. Lee, S.-H. Baek, C.B. Park, Y.-S. Bae, The immune-stimulating peptide WKYMVm has therapeutic effects against ulcerative colitis, Exp. Mol. Med. 45 (9) (2013) e40-e40.

[9] S. Bozinovski, D. Anthony, R. Vlahos, Targeting pro-resolution pathways to combat chronic inflammation in COPD, J. Thorac. Dis. 6 (11) (2014) 1548−1556.

[10] M.G. Duvall, B.D. Levy, DHA- and EPA-derived resolvins, protectins, and maresins in airway inflammation, Eur. J. Pharmacol. 785 (2016) 144−155.

[11] L. Possebon, S.S. Costa, H.R. Souza, L.R. Azevedo, M. Sant'Ana, M.M. Iyomasa-Pilon, S.M. Oliani, A.P. Girol, Mimetic peptide AC2-26 of annexin A1 as a potential therapeutic agent to treat COPD, Int. Immunopharm. 63 (2018) 270−281.

[12] L. Crocetti, C. Vergelli, G. Guerrini, N. Cantini, L.N. Kirpotina, I.A. Schepetkin, M.T. Quinn, C. Parisio, L. Di Cesare Mannelli, C. Ghelardini, M.P. Giovannoni, Novel formyl peptide receptor (FPR) agonists with pyridinone and pyrimidindione scaffolds that are potentially useful for the treatment of rheumatoid arthritis, Bioorg. Chem. 100 (2020), 103880.

[13] W. Kao, R. Gu, Y. Jia, X. Wei, H. Fan, J. Harris, Z. Zhang, J. Quinn, E.F. Morand, Y.H. Yang, A formyl peptide receptor agonist suppresses inflammation and bone damage in arthritis, Br. J. Pharmacol. 171 (17) (2014) 4087−4096.

[14] R.A. Whittington, E. Planel, N. Terrando, Impaired resolution of inflammation in alzheimer's disease: a review, Front. Immunol. 8 (2017) 1464.

[15] M.L. Stama, E. Lacivita, L.N. Kirpotina, M. Niso, R. Perrone, I.A. Schepetkin, M.T. Quinn, M. Leopoldo, Functional N-formyl peptide receptor 2 (FPR2) antagonists based on the ureidopropanamide scaffold have potential to protect against inflammation-associated oxidative stress, ChemMedChem 12 (22) (2017) 1839−1847.

[16] A.C. Martini, T. Berta, S. Forner, G. Chen, A.F. Bento, R.-R. Ji, G.A. Rae, Lipoxin A4 inhibits microglial activation and reduces neuroinflammation and neuropathic pain after spinal cord hemisection, J. Neuroinflammation 13 (1) (2016) 75.

[17] M.L. Stama, J. Slusarczyk, E. Lacivita, L.N. Kirpotina, I.A. Schepetkin, K. Chamera, C. Riganti, R. Perrone, M.T. Quinn, A. Basta-Kaim, M. Leopoldo, Novel ureidopropanamide based N-formyl peptide receptor 2 (FPR2) agonists with potential application for central nervous system disorders characterized by neuroinflammation, Eur. J. Med. Chem. 141 (2017) 703−720.

[18] K.M. Druey, Regulation of G-protein-coupled signaling pathways in allergic inflammation, Immunol. Res. 43 (1−3) (2009) 62−76.

[19] M. Arita, T. Ohira, Y.P. Sun, S. Elangovan, N. Chiang, C.N. Serhan, Resolvin E1 selectively interacts with leukotriene B4 receptor BLT1 and ChemR23 to regulate inflammation, J. Immunol. 178 (6) (2007) 3912−3917.

[20] C.B. Clish, K. Gronert, C.N. Serhan, Local and systemic delivery of an aspirin-triggered lipoxin stable analog inhibits neutrophil trafficking, Ann. N. Y. Acad. Sci. 905 (2000) 274−278.

[21] C.B. Clish, J.A. O'Brien, K. Gronert, G.L. Stahl, N.A. Petasis, C.N. Serhan, Local and systemic delivery of a stable aspirin-triggered lipoxin prevents neutrophil recruitment in vivo, Proc. Natl. Acad. Sci. Unit. States Am. 96 (14) (1999) 8247−8252.

[22] V. Kain, J.K. Jadapalli, B. Tourki, G.V. Halade, Inhibition of FPR2 impaired leukocytes recruitment and elicited non-resolving inflammation in acute heart failure, Pharmacol. Res. 146 (2019) 104295.

[23] C.N. Serhan, J.F. Maddox, N.A. Petasis, I. Akritopoulou-Zanze, A. Papayianni, H.R. Brady, S.P. Colgan, J.L. Madara, Design of lipoxin A4 stable analogs that block transmigration and adhesion of human neutrophils, Biochemistry 34 (44) (1995) 14609−14615.

[24] M.A. Sugimoto, J.P. Vago, M.M. Teixeira, L.P. Sousa, Annexin A1 and the resolution of inflammation: modulation of neutrophil recruitment, apoptosis, and clearance, J. Immunol. Res. 2016 (2016), 8239258.

[25] J.F. Maddox, M. Hachicha, T. Takano, N.A. Petasis, V.V. Fokin, C.N. Serhan, Lipoxin A4 stable analogs are potent mimetics that stimulate human monocytes and THP-1 cells via a G-protein-linked lipoxin A4 receptor, J. Biol. Chem. 272 (11) (1997) 6972−6978.

[26] K.C. Nicolaou, B.E. Marron, C.A. Veale, S.E. Webber, S.E. Dahlen, B. Samuelsson, C.N. Serhan, Identification of a novel 7-cis-11-trans-lipoxin A4 generated by

human neutrophils: total synthesis, spasmogenic activities and comparison with other geometric isomers of lipoxins A4 and B4, Biochim. Biophys. Acta 1003 (1) (1989) 44—53.

[27] T.P. O'Sullivan, K.S. Vallin, S.T. Shah, J. Fakhry, P. Maderna, M. Scannell, A.L. Sampaio, M. Perretti, C. Godson, P.J. Guiry, Aromatic lipoxin A4 and lipoxin B4 analogues display potent biological activities, J. Med. Chem. 50 (24) (2007) 5894—5902.

[28] R.R. Hodges, D. Li, M.A. Shatos, J.A. Bair, M. Lippestad, C.N. Serhan, D.A. Dartt, Lipoxin A4 activates ALX/FPR2 receptor to regulate conjunctival goblet cell secretion, Mucosal Immunol. 10 (1) (2017) 46—57.

[29] L.V. Norling, J. Dalli, R.J. Flower, C.N. Serhan, M. Perretti, Resolvin D1 limits polymorphonuclear leukocyte recruitment to inflammatory loci: receptor-dependent actions, Arterioscler. Thromb. Vasc. Biol. 32 (8) (2012) 1970—1978.

[30] S.K. Orr, R.A. Colas, J. Dalli, N. Chiang, C.N. Serhan, Proresolving actions of a new resolvin D1 analog mimetic qualifies as an immunoresolvent, Am. J. Physiol. Lung Cell Mol. Physiol. 308 (9) (2015) L904—L911.

[31] J. Pirault, M. Bäck, Lipoxin and resolvin receptors transducing the resolution of inflammation in cardiovascular disease, Front. Pharmacol. 9 (1273) (2018).

[32] T.L.Z. Wang, M.E. Cvijic, et al., Measurement of β-arrestin recruitment for GPCR targets, in: Assay Guidance Manual [Internet], Eli Lilly & Company and the National Center for Advancing Translational Sciences, 2017.

[33] T. Christophe, A. Karlsson, C. Dugave, M.J. Rabiet, F. Boulay, C. Dahlgren, The synthetic peptide Trp-Lys-Tyr-Met-Val-Met-NH2 specifically activates neutrophils through FPRL1/lipoxin A4 receptors and is an agonist for the orphan monocyte-expressed chemoattractant receptor FPRL2, J. Biol. Chem. 276 (24) (2001) 21585—21593.

[34] O. Corminboeuf, X. Leroy, FPR2/ALXR agonists and the resolution of inflammation, J. Med. Chem. 58 (2) (2015) 537—559.

[35] H.Q. He, R.D. Ye, The formyl peptide receptors: diversity of ligands and mechanism for recognition, Molecules 22 (3) (2017).

[36] R.D. Ye, F. Boulay, J.M. Wang, C. Dahlgren, C. Gerard, M. Parmentier, C.N. Serhan, P.M. Murphy, International union of basic and clinical pharmacology. LXXIII. Nomenclature for the formyl peptide receptor (FPR) family, Pharmacol. Rev. 61 (2) (2009) 119—161.

[37] G. Leoni, O. Soehnlein, (Re) solving repair after myocardial infarction, Front. Pharmacol. 9 (2018), 1342-1342.

[38] S. Bena, V. Brancaleone, J.M. Wang, M. Perretti, R.J. Flower, Annexin A1 interaction with the FPR2/ALX receptor: identification of distinct domains and downstream associated signaling, J. Biol. Chem. 287 (29) (2012) 24690—24697.

[39] T.M. Stepniewski, S. Filipek, Non-peptide ligand binding to the formyl peptide receptor FPR2–A comparison to peptide ligand binding modes, Bioorg. Med. Chem. 23 (14) (2015) 4072—4081.

[40] H.Q. He, E.L. Troksa, G. Caltabiano, L. Pardo, R.D. Ye, Structural determinants for the interaction of formyl peptide receptor 2 with peptide ligands, J. Biol. Chem. 289 (4) (2014) 2295—2306.

[41] T. Chen, M. Xiong, X. Zong, Y. Ge, H. Zhang, M. Wang, G. Won Han, C. Yi, L. Ma, R.D. Ye, Y. Xu, Q. Zhao, B. Wu, Structural basis of ligand binding modes at the human formyl peptide receptor 2, Nat. Commun. 11 (1) (2020) 1208.

[42] Y. Asahina, N.R. Wurtz, K. Arakawa, N. Carson, K. Fujii, K. Fukuchi, R. Garcia, M.Y. Hsu, J. Ishiyama, B. Ito, E. Kick, J. Lupisella, S. Matsushima, K. Ohata, J. Ostrowski, Y. Saito, K. Tsuda, F. Villarreal, H. Yamada, T. Yamaoka, R. Wexler, D. Gordon, Y. Kohno, Discovery of BMS-986235/LAR-1219: a potent formyl peptide receptor 2 (FPR2) selective agonist for the prevention of heart failure, J. Med. Chem. 63 (17) (2020) 9003—9019.

[43] A.K. Stalder, D. Lott, D.S. Strasser, H.G. Cruz, A. Krause, P.M. Groenen, J. Dingemanse, Biomarker-guided clinical development of the first-in-class anti-inflammatory FPR2/ALX agonist ACT-389949, Br. J. Clin. Pharmacol. 83 (3) (2017) 476—486.

[44] W. Huang, A. Manglik, A.J. Venkatakrishnan, T. Laeremans, E.N. Feinberg, A.L. Sanborn, H.E. Kato, K.E. Livingston, T.S. Thorsen, R.C. Kling, S. Granier, P. Gmeiner, S.M. Husbands, J.R. Traynor, W.I. Weis, J. Steyaert, R.O. Dror, B.K. Kobilka, Structural insights into micro-opioid receptor activation, Nature 524 (7565) (2015) 315—321.

[45] G. Pándy-Szekeres, C. Munk, T.M. Tsonkov, S. Mordalski, K. Harpsøe, A.S. Hauser, A.J. Bojarski, D.E. Gloriam, GPCRdb in 2018: adding GPCR structure models and ligands, Nucleic Acids Res. 46 (D1) (2017) D440—D446.

[46] R.W. Burli, H. Xu, X. Zou, K. Muller, J. Golden, M. Frohn, M. Adlam, M.H. Plant, M. Wong, M. McElvain, K. Regal, V.N. Viswanadhan, P. Tagari, R. Hungate, Potent hFPRL1 (ALXR) agonists as potential anti-inflammatory agents, Bioorg. Med. Chem. Lett 16 (14) (2006) 3713—3718.

[47] J. Ostrowski, Ricardo Wurtz Garcia, R. Nicholas, Targeting of the Formyl-Peptide Receptor 2/Lipoxin A4 Receptor (FPR2/ALX) for Treatment of Heart Disease. WO2017091496, 2017.

[48] R.L. Beard, J.E. Donello, V. Wiswanath, Use of Agonists of Formyl Peptide Receptor 2 for Treating Ocular Inflammatory Diseases. WO20170320897, 2017.

[49] R.L. Beard, T. Duong, J.E. Donello, V. Viswanath, M.E. Garst, (2-ureidoacetamido)alkyl Derivatives as Formyl Peptide Receptor 2 Modulators. WO20130274230, 2013.

[50] R.L. Beard, T.T. Duong, J.E. Donello, V. Viswanath, M.E. Garst, Amide Derivatives of N-Urea Substituted Amino Acids as Formyl Peptide Receptor Like-1 (Fprl-1) Receptor Modulators. WO2013062947, 2013.

[51] V. Viswanath, R.L. Beard, J.E. Donello, E.C. Hsia, Use of Agonists of Formyl Peptide Receptor 2 for Treating Dermatological Diseases, 2014. WO/2014/138046.

[52] D. Bur, O. Corminboeuf, S. Cren, H. Fretz, C. Grisostomi, X. Leroy, J. Pothier, Aminopyrazole Derivatives, 2009. WO2009077954.

[53] D. Bur, O. Corminboeuf, S. Cren, C. Grisostomi, S. Richard-Bildstein, Oxazolyl-methylether Derivatives as ALX Receptor Agonists, 2012. WO2012077049.

[54] D. Bur, O. Corminboeuf, S.G.C. Cren, X. Leroy, D. Pozzi, S. Richard-Bildstein, Hydroxylated Aminotriazole Derivatives as ALX Receptor Agonists, 2012. WO2012077051.

[55] K. Fujii, Kentaro Umei, Hiroyasu Takahashi, Mitsuhito Shibasaki, Kohei Ohata, Urea Derivative or Pharmacologically Acceptable Salt Thereof, 2016. WO2016189876.

[56] D. Bur, O. Corminboeuf, S. Cren, C. Grisostomi, X. Leroy, D. Pozzi, S. Richard-Bildstein, Bridged spiro[2.4]heptane Ester Derivatives, 2012. WO2012066488.

[57] D. Bur, O. Corminboeuf, S. Cren, C. Grisostomi, X. Leroy, S. Richard-Bildstein, Bridged Spiro [2.4] Heptane Derivatives as ALX Receptor And/Or FPR2 Agonists. WO2010134014, 2010.

[58] O. Corminboeuf, S. Cren, 1-(p-tolyl)cyclopropyl Substituted Bridged spiro[2.4] heptane Derivatives as ALX Receptor Agonists, 2013. WO2013171687.

[59] M.P. Giovannoni, I.A. Schepetkin, A. Cilibrizzi, L. Crocetti, A.I. Khlebnikov, C. Dahlgren, A. Graziano, V. Dal Piaz, L.N. Kirpotina, S. Zerbinati, C. Vergelli, M.T. Quinn, Further studies on 2-arylacetamide pyridazin-3(2H)-ones: design, synthesis and evaluation of 4,6-disubstituted analogs as formyl peptide receptors (FPRs) agonists, Eur. J. Med. Chem. 64 (2013) 512—528.

[60] I.A. Schepetkin, L.N. Kirpotina, A.I. Khlebnikov, M. Leopoldo, E. Lucente, E. Lacivita, P. De Giorgio, M.T. Quinn, 3-(1H-indol-3-yl)-2-[3-(4-nitrophenyl) ureido]propanamide enantiomers with human formyl-peptide receptor agonist activity: molecular modeling of chiral recognition by FPR2, Biochem. Pharmacol. 85 (3) (2013) 404—416.

[61] L.N. Kirpotina, A.I. Khlebnikov, I.A. Schepetkin, R.D. Ye, M.J. Rabiet, M.A. Jutila, M.T. Quinn, Identification of novel small-molecule agonists for human formyl peptide receptors and pharmacophore models of their recognition, Mol. Pharmacol. 77 (2) (2010) 159—170.

[62] R.L. Beard, Tien T. Duong, Michael E. Garst, Phenylcarbamate Derivatives as Formyl Peptide Receptor Modulators. WO2015077451, 2015.

[63] S. Yamamoto, J. Shirai, M. Kouno, Y. Tomata, A. Sato, A. Ochida, Y. Fukase, S. Fukumoto, T. Oda, H. Tokuhara, N. Ishii, Y. Sasaki, Amide Compound, 2015. WO2015002230.

[64] M.P. Dwyer, K.M. Keertikar, Q. Zeng, R.D. Mazzola Jr., W. Yu, H. Tang, S.H. Kim, L. Tong, S.B. Rosenblum, J.A. Kozlowski, A.G. Nair, Silyl-Containing Heterocyclic Compounds and Methods of Use Thereof for the Treatment of Viral Diseases, 2013. WO2013039876.